Thesis

Insights into Aortic Dissection: From Clinical Perspectives to Advanced Imaging and Segmentation Techniques

A Comprehensive Study on Aortic Dissection with a Focus on Stanford Type B Segmentations

submitted by

Sophie Hossain

in partial fulfillment of the requirements for the degree of

Doktorin der gesamten Heilkunde

(Dr. med. univ.)

at the

Medical University of Graz

executed at the University departments of

Klin. Abteilung für Herzchirurgie, Universitäres Herzzentrum Graz

under the supervision of

Ao.Univ.Prof. Dr. Heinrich Mächler, MSc, MBA und

Univ.Ass, Dr. Christian Mayer

Graz, 25.07.24

Declaration of Academic Integrity

I hereby confirm that the present diploma thesis is the result of my own independent scholarly works. I also confirm that in all cases, where material from the work of others (in books, articles, essays, dissertations, and on the internet) is acknowledged, quotations and paraphrases are clearly indicated. No material other than that cited in the reference list has been used. I have read and understood the Medical University's regulations and procedures concerning plagiarism.

Graz, 25.07.24 Sophie Hossain m.p.

Acknowledgements

I extend my heartfelt thanks to Professor Dr. Heinrich Mächler and Dr. Christian Mayer for their invaluable support, guidance, and scholarly input throughout the completion of this thesis. Their expertise and meticulous correction of medical aspects have greatly enriched this work.

I am also deeply thankful to my sister Anne Hossain and aunt Ulrike Rüb-Taylor for their assistance in improving the English language aspects of this thesis.

Furthermore, I am grateful to my parents and friends for their unwavering moral support throughout this journey. Their encouragement was a constant source of strength and motivation.

Thank you all for believing in me and contributing to the successful completion of this endeavor.

Zusammenfassung

Die Aorta ist die größte Arterie im menschlichen Körper und das Hauptgefäß für den Transport von sauerstoffreichem Blut. Deshalb spielt sie eine entscheidende Rolle bei der Aufrechterhaltung des kardiovaskulären Kreislaufes. Die strukturelle Integrität der Aortenwand kann aus verschiedenen Gründen beeinträchtigt werden und zu einer Erkrankung führen, die als Aortendissektion (AD) bekannt ist. Die Aortendissektion ist eine potenziell lebensbedrohliche Erkrankung, die durch das Einreißen einzelner Schichten der Aortenwand gekennzeichnet ist. Diese Trennung der Wandschichten führt zur Bildung eines falschen Lumens innerhalb des Gefäßes [46, 47].

Der erste Teil dieser Diplomarbeit zielt darauf ab, einen zusammenfassenden Überblick über die Erkrankung Aortendissektion zu bieten. Dabei ist eine detaillierte Betrachtung der Definition, Pathologie, Pathophysiologie, klinischen Manifestationen, diagnostischen Ansätze und therapeutischen Optionen, eingeschlossen. Anhand von Organisation und Erklärung der verschiedenen Aspekte von Aortendissektionen wird diese Diplomarbeit die Komplexitäten der AD beleuchten und so eine verbesserte klinische Betreuung und bessere Ergebnisse für Patientinnen und Patienten ermöglichen.

Der Einsatz von Bildgebungstechniken wie die Computertomographie mit Angiographie (CTA) unterstützt die Diagnose und das Management von Aortendissektionen. Jedoch hat die Integration von algorithmischen Softwares und fortschrittlichen Bildgebungstechniken für die Verfahrensplanung in den letzten Jahren zunehmend an Bedeutung gewonnen, da dreidimensionale (3D) Bildgebungstechniken eine präzisere und detailliertere Visualisierung der Aortenanatomie ermöglichen. Insbesondere bei der Planung komplexer Verfahren für Patientinnen und Patienten mit Aortenerkrankungen wie der Stanford Typ B Aortendissektion und der klinischen Entscheidungsfindung spielt eine schnelle und präzise visuelle Beurteilung eine entscheidende Rolle [29, 52, 55].

Aus diesem Grund zielt der zweite Teil der Diplomarbeit darauf ab, die Nutzung von 3D-Bildgebungstechniken bei der Diagnose und dem Management von Typ-B-Aortendissektionen zu untersuchen. Die Diplomarbeit konzentriert sich zunächst auf die Sammlung von 40 Fällen und die Konvertierung von CTA-Scans in ein anonymes Format. Anschließend erfolgte die Erkundung verschiedener Open-Source-Softwareprogramme und Segmentierungsmethoden. Die Segmentierung und Analyse von Typ-B-

Aortendissektionen wurde mittels der Open-Source-Software "3DSlicer" durchgeführt. Dabei wurde sowohl das wahre, als auch das falsche Lumen berücksichtigt und 16 CTA-Scans konnten erfolgreich von der Autorin segmentiert werden. Die Prozessbeschreibung schließt mit der detaillierten Erklärung dieser 16 Fälle ab.

Mit den Segmentierungen kann in weiterer Folge ein „Ground-Truth“-Datensatz erstellt werden, der für das Training und die Bewertung zukünftiger KI-Algorithmen unerlässlich ist, um automatisierte Segmentierungsprogramme zu entwickeln. Der anonymisierte Datensatz enthält keine patientenspezifischen Daten und kann daher von multidisziplinären Teams und Technikern verwendet werden. Es können KI-Algorithmen entwickelt werden, die durch fortschrittliche 3D-Modellierung potenziell erhebliche klinische und zeitliche Vorteile für Patientinnen und Patienten mit Aortendissektion bieten [52, 55].

Zusammenfassend leistet diese Diplomarbeit wertvolle Beiträge zum Verständnis der Aortendissektion als Krankheit und bietet eine umfassende Untersuchung des Segmentierungsprozesses von 16 Fällen mit Typ B Aortendissektionen. Die Anwendung der Open-Source-Software „3DSlicer“ für die Segmentierung stellt einen bedeutenden Fortschritt dar und zeigt zukünftiges Potenzial für verbesserte Diagnostik und Verständnis im Bereich der Herzchirurgie, sowie eine optimierte Versorgung von Patientinnen und Patienten mit Aortenerkrankungen.

Abstract

The aorta is the largest artery in the human body and the body's primary conduit for oxygenated blood. Therefore, it plays a crucial role in maintaining cardiovascular health. However, the structural integrity of the aortic wall can be compromised for various reasons, leading to a condition known as aortic dissection (AD). Aortic dissection is a potentially life-threatening condition that affects the aorta and is characterized by a tear of the aortic wall. This separation of layers of the aortic wall results in the formation of a false lumen within the vessel [46, 47].

The first part of this thesis aims to provide a comprehensive exploration of aortic dissection, including a detailed examination of its definition, pathology, pathophysiology, clinical manifestations, diagnostic approaches, and therapeutic options. By exploring and organizing the diverse aspects of aortic dissections, this thesis will elucidate the complexities surrounding the nature of AD, facilitating improved clinical management and patient outcomes.

Imaging techniques, such as computed tomography with angiography (CTA), aid in the diagnosis and management of aortic dissection. However, the integration of algorithmic software and advanced imaging techniques for procedural planning has become increasingly important in recent years, as three-dimensional (3D) imaging techniques allow for a more precise and detailed visualization of aortic anatomy. Subsequently, it enables more precise and prompt diagnoses, while also facilitating the planning of surgical interventions. Especially in the planning of complex procedures for individuals with aortic conditions, such as Stanford type B aortic dissection, a quick and accurate visual assessment plays a critical role in clinical decision making [29, 52, 55].

Therefore, the second part aims to investigate the use of 3D imaging techniques in the diagnosis and management of type B aortic dissections. Specifically, this thesis focuses on collecting 40 cases and converting CTA scans into an anonymous format. Subsequently, various open-source software programs were explored and several segmentation methods were tested using the open-source software "3DSlicer".Thereby, both the true and false lumen were included, and 16 CTA scans were successfully segmented by the author. The process description concludes with an explanation of these 16 cases.

Using these segmentations a "ground-truth" dataset for training and assessing future AI algorithms can be created, which is crucial for developing automated segmentation

programs. Due to the time-consuming nature of the semi-automatic segmentation process, automation can significantly enhance decision making and therapy for patients with aortic dissection. The anonymized dataset does not contain patient-specific data and can therefore be published for multidisciplinary teams and technicians to develop AI algorithms. These algorithms potentially offer substantial clinical benefits through advanced 3D-modeling [52, 55].

In conclusion, this thesis contributes valuable insights into aortic dissection as a disease and provides an analysis through a comprehensive examination of 16 cases. The application of the open-source software "3DSlicer" for segmentation proves to be a significant advancement, showcasing future potential for enhanced diagnostics and understanding in the field of cardiac surgery, and optimized patient care for aortic diseases.

Publications in connection with the project of this thesis

- Mayer C, Pepe A, **Hossain S,** Karner B, Arnreiter M, Kleesiek J. Type B Aortic Dissection CTA Collection with True and False Lumen Expert Annotations for the Development of AI-based Algorithms. Nature, Sci Data. 2024;11:596.
- Mayer C, Arnreiter M, Karner B, **Hossain S,** Deutschmann HA, Zimpfer D. Aortic Segmentations and Their Possible Clinical Benefits. In: Segmentation of the Aorta. Towards the Automatic Segmentation, Modeling, and Meshing of the Aortic Vessel Tree from Multicenter Acquisition. 2024 p. 135-140. doi:10.1007/978-3-031-53241-2_11.
- Pepe A, Li J, Rolf-Pissarczyk M, Gsaxner C, Chen X, Holzapfel G. Detection, Segmentation, Simulation and Visualization of Aortic Dissections: A Review. Med Image Anal. 2020. doi:10.1016/j.media.2020.101773.

Abstracts:

- Arnreiter M, Karner B, Mayer C, **Hossain S,** Pepe A, Mächler H. Utilizing Three-Dimensional Image Segmentation for Swift Evaluation of Morphology and Risk Classification in Type B Aortic Dissection. Abstract Grazer Herzkreislauftage. 2023.
- Karner B, Arnreiter M, Mayer C, **Hossain S,** Mächler H, Deutschmann HA, et al. Three-dimensional Image Segmentation Permits Rapid Morphologic Assessment and Risk Stratification in Type B Aortic Dissection. Abstract ÖGHTG. 2023.
- Mayer C, Pepe A, **Hossain S,** Karner B, Arnreiter M, Mächler H, et al. Segmentation of Type B Aortic Dissections with True and False Lumen for the Development of AI-based Algorithms. Abstract ÖGHTG. 2023.

Table of content

Index of abbreviations

AD……..……Aortendissektion/ Aortic Dissection

CT……Computed tomography

CTA…..Computertomographie mit Angiographie/ Computed tomography with angiography

3D……..……Dreidimensional/ Three-dimensional

TL……...……True lumen

FL……..……False lumen

HU……..……...Hounsfield Units

SD……...……Standard deviation

MRT……...……Magnetic resonance tomograph

MRI……Magnetic resonance imaging

MRA……...…Magnetic resonance imaging with angiography

AI……...…….Artificial intelligence

PAU……...……Penetrating atherosclerotic ulcer

LSA……..……Left Subclavian Artery

TC……Truncus coeliacus

AMS……Arteria mesenterica superior

ISA…….……...Intrinsic sympathomimetic activity

TEVAR…….……Thoracic endovascular aortic repair

MUG……..……Medical university of Graz

NRRD……..……...Nearly Raw Raster Data

DICOM……...……...Communications in Medicine

mm……..…...……Millimetres

cm³……...……Cubic centimetres

ST…….……..Segmentation time

SM…….……Segmentation method

AscAo…….……Ascending aorta

Index of figures

Index of tables

Part I: Theory

1. Introduction

The aorta is the largest artery in the human body and the body's primary conduit for oxygenated blood. Therefore, it plays a crucial role in maintaining cardiovascular health. However, the structural integrity of the aortic wall can be compromised for various reasons, leading to a condition known as aortic dissection (AD). Aortic dissection is a potentially life-threatening condition that affects the aorta and is characterized by a tear of the aortic wall. This separation of layers of the aortic wall results in the formation of a false lumen within the vessel. A variety of serious complications can arise in this condition, including aortic rupture, organ malperfusion, and even death [46, 47].

The clinical significance of aortic dissections lies not only in their sudden onset, but also in the complexity of their pathophysiology and the diverse range of presenting symptoms. Aortic dissections are relatively rare, affecting approximately 2-3 per 100, 000 people per year. However, the mortality rate is high, ranging from 20-50% within the first 48 hours without appropriate treatment [58].

By exploring and organizing the diverse aspects of aortic dissections, this thesis will elucidate the complexities surrounding the nature of AD, facilitating improved clinical management and patient outcomes. Therefore, this thesis contributes to a deeper understanding of this potentially life-threatening cardiovascular disorder.

The Stanford classification of aortic dissection is commonly used and is based on the involvement of the ascending aorta, with Type A dissections beginning in the ascending aorta and Type B dissections starting after the left subclavian artery. Risk factors for aortic dissection include hypertension, smoking, atherosclerosis, connective tissue disorders, and genetic predisposition [1, 46].

The clinical presentation and symptoms of aortic dissection depend on the location and extent of the tear, and can therefore vary. However, AD typically includes a sudden onset of severe chest or back pain, which may radiate to the neck, arms, or legs [47].

While there are various methods for diagnosing aortic dissection, such as magnetic resonance tomography (MRT) or thoracic X- Ray, the gold standard is computed tomography angiography (CTA) [27].

The treatment of aortic dissection differs between the different types. While type A aortic dissections are primarily treated surgically, uncomplicated type B dissections are often treated conservatively. In general, the goal is to reduce blood pressure, repair the aortic wall, decrease the risk of further tearing, and prevent complications [27]. Advanced imaging techniques, such as CTA, can aid in the diagnosis and management of aortic dissection.

2. Definition

2.1 Aortic Anatomy

The aorta is the main central artery in the human body. It originates in the heart and transports oxygenated blood to the body´s periphery. The aortic valve separates the aorta from the left ventricle. The aorta can be divided into separate anatomical segments commencing with the aortic root, including the coronary sinuses, which is directly connected to the heart. The following part is called ascending aorta, then continuing as the aortic arch, where the artery changes its direction to dorsal and caudal. It includes the vascular branches Truncus brachiocephalicus, Arteria carotis communis sinistra, and Arteria subclavia sinistra. The following part is called descending aorta, which includes intercostal arteries and various smaller branches. The part of the aorta starting from the aortic root up to the diaphragm, including all the mentioned segments, is referred to as the thoracic aorta or pars thoracica. As the aortic hiatus, the passage through the diaphragm, is considered a border, the distal following passage is designated as the abdominal aorta or pars abdominalis. Immediately after the diaphragm, several branches diverge from the aorta to supply blood to visceral organs and kidneys. Subsequently, the abdominal aorta separates into the aortic bifurcation of the two arteriae iliacae communes [18, 52].

The aortic wall is composed of three distinct layers, each with its own structure and function.

1. **Tunica Intima**: The innermost layer is called the tunica intima, which consists of a single layer of endothelial cells that surround the lumen of the aorta, providing a smooth surface for blood flow. Beneath the endothelial layer is a thin layer of connective tissue and an internal elastic lamina enabling flexibility.

   Membrana elastica interna, a membrane of elastic fibers.

2. **Tunica Media**: The middle layer, the tunica media, is the thickest and most robust layer and is composed mainly of smooth muscle cells and elastic fibers. Smooth

muscle inserts into fibrillin microfibrils within the lamellae, connecting them at an oblique angle. These connections are inherently weaker than lamellae, making them the most susceptible position for tears. Furthermore, the direction of the tear can change when the lamellae connect [5]. Since the aorta needs to adapt to many different and rapidly changing volumes, the middle layer contains many elastic fibers. Therefore, the "Wind Kessel effect" in the aorta exists. This effect refers to the elastic properties of the arterial wall, allowing it to expand during systole, store kinetic energy, and subsequently recoil during diastole, facilitating continuous and smooth blood flow [50].

Membrana elastica externa, a membrane of elastic fibers.

3. **Tunica Adventitia**: The outermost layer, the tunica adventitia, is composed of connective tissue that contains collagen and elastic fibers. It provides additional support and structure to the aorta and houses small blood vessels (vasa vasorum) that supply blood to the walls of large arteries as well as nerve fibers [21].

2.2 Aortic Dissection

An aortic dissection (AD) is defined as an acute tear in the already mentioned innermost layer of the aortic wall, the Intima. Through this tear, blood can enter the middle part of the wall, creating a second lumen between the inner and outer layers of the wall, and effectively separating them. This lumen inside the wall is the so named „false“ lumen and is filled with

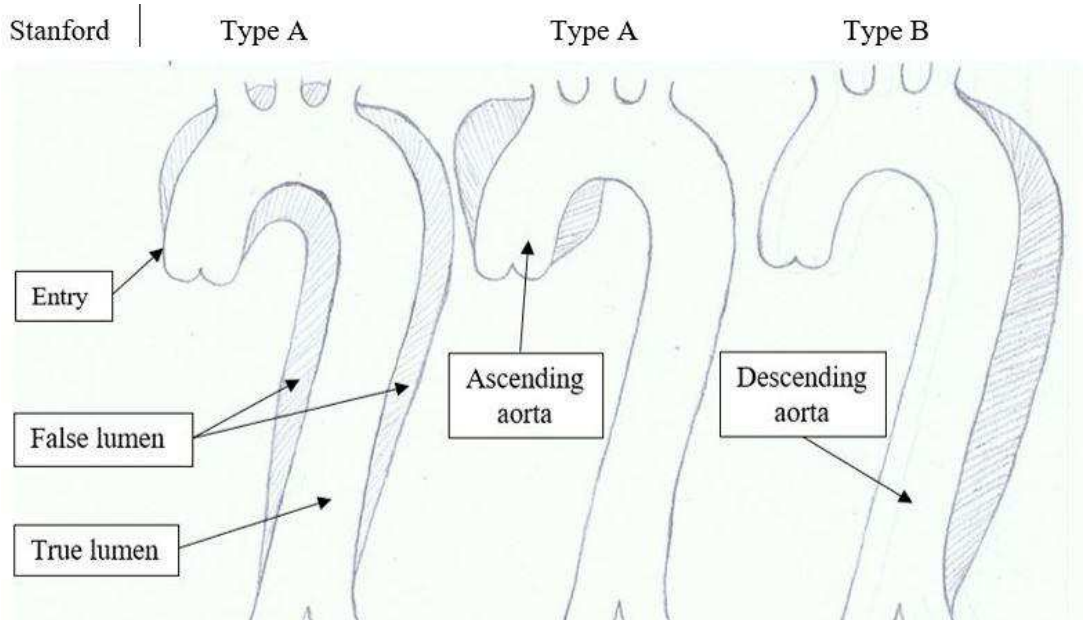

Figure 1: Types of aortic dissection separated by entry (Stanford), source: Author

blood expanding within the layers [58]. In the early phase of dissection, intramural hematoma with or without progression to dissection is possible.

As shown in Figure 1, aortic dissection can be classified into two distinct types: Stanford types A and B. The Stanford classification was introduced in 1970, and is the most frequently used classification. The crucial point in this classification is not the position of the tear but whether it extends into the ascending aorta. However, the length of the dissection or created false lumen is not relevant. A dissection that affects both the aortic arch and the descending aorta but excludes the ascending aorta is classified as non-A non-B. [1]. However, this non-A non-B type is not discussed further in this thesis. As described in more detail later, dissection can cause myocardial infarction, stroke, intestinal ischemia, and hypoperfusion of the causal extremities, depending on the position. Other classifications, such as the three Bakey types, are rudimentary and not commonly used clinically.

As indicated in Figure 1, Stanford Type A aortic dissections involve a tear primarily in the Tunica intima within the ascending aorta. According to Gudbjartsson [1], it is crucial to note that the Stanford classification does not specifically classify tear sites. Consequently, an intimal tear distal to the left subclavian artery with retrograde dissection into the ascending aorta is categorized as Type A or non-A non-B type [1 p2 l12]. The dissection may remain localized in this region but typically extends to the descending part or even the entire length of the aorta. Type A dissections are much more prevalent, accounting for approximately 50 percent in the ascending and 5-10 percent in the aortic arch, with the remaining 40% being Stanford Type B dissections. Cases of Stanford A dissection represent a life-threatening emergency with a high mortality rate within the first 48 hours [20].

Stanford type B dissections describe dissections starting distal to the arteria subclavia sinistra in the descending aorta. Similar to type A dissection, the second lumen can extend further into the abdominal aorta. It occurs less frequently and since the intravascular blood pressure in the descending part is not as high, the risk of sudden rupture is lower. While Stanford A cases are mostly acute and in need of a quick intervention, Stanford B dissections can be separated into “complicated” in need of treatment and “uncomplicated”, without the need for treatment. Chronic aortic dissection is a slowly progressing aortic disease.

3. Pathology

3.1 Epidemiology

The frequency of aortic dissection is approximately 2-3 per 100.000 persons per year, with an average age of over 50 years. An exception are tissue diseases such as Marfan- Syndrome, which has a peak incidence at 30 years. The sex distribution is three males to one female [58]. Similar to many other diseases, differences exist between the sexes and cultures. Differences in perception and communication of pain contribute to challenges in making a correct and fast diagnosis. In general, aortic dissection is more frequently observed in men, who commonly exhibit typical symptoms of acute chest pain radiating to the back. Conversely, women may occasionally present with less typical symptoms, such as complications involving the heart or altered mental status [6]. “In the past several decades, there has been a notable increase in reported incidence of thoracic aortic disease - though it is unclear if this is a consequence of better diagnostic imaging, disease recognition, or a true change in disease epidemiology” [6 p2]. In addition to Stanford’s anatomical classification, aortic dissection can be separated by cause. It is worth noting that preexisting ascending aneurysms are a major cause of type A dissection. The enlarged diameter of the ascending aorta increases the susceptibility to dissection compared with the normal diameter. Therefore, the subsequent risk factors and causes are not only relevant to the development of aortic dissection but also to aortic aneurysms.

3.2 Acquired aortic dissection: Risk factors

The primary causes of aortic dissection are underlying diseases and the consequences of an unhealthy lifestyle, including hypertension and atherosclerosis. All these factors can cause damage to the vascular walls. Atherosclerosis is the most frequent form of blood-vessel damage.

Both atherosclerosis and hypertension carry a high risk for aortic aneurysms. This pathological extension of the aorta, including all layers of the wall, is a sign of a weakened vessel and increases the risk of rupture and aortic dissection. In addition, a penetrating aortic ulcer is associated with hypertension and cigarette smoking, and arises from an atherosclerotic plaque in the vascular wall. This ulcerative defect of the inner wall penetrates through the Membrana elastica interna into the tunica media. Blood can then enter the media, causing intramural hematoma or dissection. In advanced types of atherosclerosis, the vasa vasorum of the aorta can rupture and increase the blood flow inside the hematoma. In some

cases, this hematoma remains inside the aortic wall without a connection to the lumen; other cases have shown a rise in pressure inside the wall, leading to a tear in the intima and aortic dissection or rupture [3]. Furthermore, there are variations in aortic dissection such as dissection through an intramural hematoma. Intramural hematomas can exist without a clear tear or a tear in the intima with an aneurysm, but without a false lumen. In addition, an existing hematoma, dissection, or hematoma through ulceration of atherosclerotic plaques can be considered precursors to classic aortic dissection. Similar to aortic dissection, atherosclerosis is more common in males and occurs earlier in men than in women [17]. "Data from inpatient sampling to determine the association between aortic dissection and diabetes mellitus established that diabetes type 2 was significantly and negatively associated with thoracal aortic dissection." [2 p3].

Another, rarer, lifestyle-associated cause of dissection can be drug abuse, mostly amphetamine or cocaine. The typical patient in this case would be a young male. Even though studies [4] show a connection between the use of cocaine and acute aortic dissection, it might only be a final trigger for an already damaged vascular system. Drug abuse is often associated with a history of hypertension and cigarette smoking. The pathophysiological mechanism remains unknown, but it is theorized that chronic and frequent use of these substances may lead to stiffening of arterial walls, rendering them more susceptible to damage.

3.3 Inflammatory and autoimmune causes

All the above-mentioned underlying diseases can lead to aortic dissection not only by damaging the Intima of the aorta, but also by inducing inflammation at a damaged position. Inflammation of the aorta can damage the aortic wall, leading to dissection. Possible infectious causes, include for example syphilis, bacterial endocarditis, and tuberculosis. Additionally, autoimmune sources, such as Lues or Takayasu arteritis, can also contribute. Degeneration of the aortic wall due to vasculitis or aortitis involves immunoglobulin G4 and complement 4d. Giant cells or Takayasu arteritis, however, are mostly associated with T-cell-mediated vasa vasorum [1]. For example, mucoid microcytic degeneration of the media, also known as medio necrosis Erdheim-Gsell, is not inflammatory but autoimmune degeneration. Contrary to its name, inflammation of the medium layer of the aortic wall rarely leads to necrosis, but rather to apoptosis of myocytes caused by the attachment of basophile liquid in the tunica media. Furthermore, loss of elastic and collagenous fibers

could be detected. As explained in the next category, this autosomal dominant inherited disease is often associated with other inherited diseases such as Marfan syndrome.

3.4 Inherited or genetic causes

Aortic dissection is less common in young patients, necessitating exploration of causes beyond atherosclerosis or degeneration. Genetic or inherited diseases can result in damage to the vascular walls. These afflictions might not be very frequent but carry a high risk of aortic dissection. According to the Nordic consortium for acute type A aortic dissection registry, nearly eight percent of patients with acute aortic syndrome have a positive family history of aortic dissection [1]. Marfan syndrome or Ehlers Danlos syndrome of the vascular type are diseases causing defects or malfunction of the connecting tissue, leading to an instability of all connecting tissues, including the stability of the vessels. Another congenital phenomenon is the bicuspid aortic valve, which consists of only two leaflets instead of three. Frequently, two of the three leaflets are fused into one, often still having a raphe visible on echocardiography. This abnormality is the most frequent congenital valve defect, shows familial clustering, and appears more frequently in males. This bicuspid valve often does not allow sufficient closure, which leads to a higher mechanical load that can further lead to a degenerative restructuring process, aortic insufficiency, aortic aneurysm, early aortic stenosis, and aortic dissection [6].

The bicuspid aortic valve can also appear in relation to other syndromes, such as Turner-syndrome. With this syndrome, one X chromosome of the female genotype is missing, causing different symptoms, malformations of different organs, and abnormalities in physical appearance. The occurrence of aortic stenosis, a narrowing of the aorta, and the bicuspid aortic valve increase the risk of aortic dissection. Other genetic or congenital syndromes related to aortic dissections include Loeys-Dietz-syndrome, Aneurysm-osteoarthritis-syndrome, and non-syndromic familial forms of thoracic aortic aneurysm [6].

3.5 Traumatic causes

The final category contributing to aortic dissection includes traumatological causes. In traumatic causes, such as blunt trauma, the aortic wall can rupture with a predominantly transverse tear rather than a longitudinal tear. Deceleration trauma, such as car accidents or falls from a great height, can induce shear stress, leading to rupture of the aortic wall. The ligamentum arteriosum, which connects the left pulmonary artery to the descending aorta, plays an important role by anchoring the aorta and limiting its mobility within the thorax.

This restriction helps restrain the aorta in cases of acceleration or displacement within the mediastinum. Consequently, rupture or injury in the isthmus region of the aorta, called transection or aortic rupture loco typico, is more likely. Depending on the situation, traumatic rupture is caused by a sudden increase in intrathoracic pressure, dislocation, or rotation of mediastinal organs, such as the ribs. While the aortic wall might rupture completely in severe trauma, local defects or aortic dissection are more frequent later on. Furthermore, it can lead to weakening of the aortic wall, which can rupture more easily later in life [5]. Rare cases also show a connection between high-intensity weightlifting and aortic dissection [58].

4. Pathophysiology

Inherited, inflammatory, traumatic, and acquired causes and conditions are all associated with aortic wall tearing. Tearing can lead to serious and potentially life-threatening conditions. The main focus of this thesis is **aortic dissection**, in which a tear in the intima, the so-called entry, allows blood to flow between the outer layers of the aortic wall. A separation of layers, a dissection, with a second, false lumen between the Intima and the Adventitia is created. While one theory assumes that a tear in the intima is the source of the dissection, others describe that the entry into the true lumen is already a consequence of the false lumen [6]. The false lumen can extend longitudinally inside the wall. The extension of the dissection depends on one hand on blood pressure and on the other hand on the resilience of the Tunica media. While some dissections are only a few millimeters long, others can extend through several centimeters or, in extreme cases, even the whole length of the aorta, including the arteries directly branching off the aorta [19]. The dissection in the aortic wall can be seen in the longitudinal cut and cross-section in figure 2.

However, there are other possible outcomes. An **intramural hematoma**, where the bleeding is within the aortic wall itself without an intimal tear, can mimic a dissection and lead to similar complications. The already mentioned **Aortic transection**, often caused by severe trauma, involves a partial or complete tear through the aorta, requiring immediate surgical intervention. Aortic **rupture** refers to a complete tear through all layers of the aortic wall, resulting in massive internal bleeding and is typically fatal if not rapidly treated. Lastly, **penetrating atherosclerotic ulcer (PAU)** occurs when atherosclerotic plaque erodes through the intima into the media, which can lead to hematoma formation, dissection, or even rupture. Each of these conditions requires prompt medical attention to prevent severe complications or death.

As per [54], the typical development of dissections can be summarized in six different stages. Based on one hypothesis, the aortic wall is exposed to stress or tissue abnormalities in the first stage. In stage two, there is an entry into the tunica media, forming a second lumen. In this stage, the blood flow is almost normal, showing only minimal disturbances, whereas the flow in the third stage is already affected. Here, there is no sign of thrombosis. The dissection, however, has already extended longitudinally through the vascular wall. The subsequent, fourth stage is characterized by the emergence of a second entry distally or another re-entry point. Through these two or more tears blood can circulate freely through both lumens. For certain patients, the fourth stage marks the final phase. In others, thrombosis, originating from the distal side of the false lumen, accumulates, resulting in the occlusion of distal tears and intramural blood flow. Consequently, the fifth stage is considered optional. In the optional sixth stage, the formed thrombus completely fills the false lumen within the wall.

In the second theory, the pathophysiology of the beginning of a dissection is not based on a tear in the intima. Instead, rupture or damage to the vasa vasorum leads to blood flow into the media. The blood creates a gap filled with blood between the layers of the wall. Consequently, the pressure on the intima wall from the hematoma increases. Additionally, there might already be damage to the vascular wall because of triggering diseases, such as atherosclerosis. Due to both, the innermost layer of the aortic wall gives in, creating an opening into the true lumen of the aorta [6]. Even though the first two stages differ in the second hypothesis of creation, further stages remain the same. However, in the second scenario, there is a higher likelihood of blood remaining within the wall, resulting in a circumscribed hematoma, as described in stage number six. Another term for this scenario is intramural hematoma.

Regardless of the original creation of the two lumina, both blood flow and blood pressure are now lower, which can cause ischaemia in arteries branching off the false lumen. As described in the later stages of the typical development [54], dissections can communicate with the true lumen of the aorta through the entry of the dissection. Consequently, dissection does not necessarily interrupt systemic blood flow. Nevertheless, in certain cases, depending on the location and extent of the false lumen, arteries branching off the aorta may receive a reduced blood supply or can be entirely deprived of blood flow, resulting in ischemia and malperfusion syndrome. In this critical situation, the associated organs or regions do not receive sufficient blood and oxygen, eventually leading to the cessation of their function. The gravity of ischemia, as explained later, depends on which arteries are affected and is far more dangerous in Stanford type A dissections. Blood flowing through the false lumen leads to an enormous increase in pressure inside the wall. Since the aortic wall is already destabilized not only through the tear but also due to the cause of the tear, high pressure in the wall can cause a second tear in the intima. This second tear re-enters the true lumen of the aorta [17].

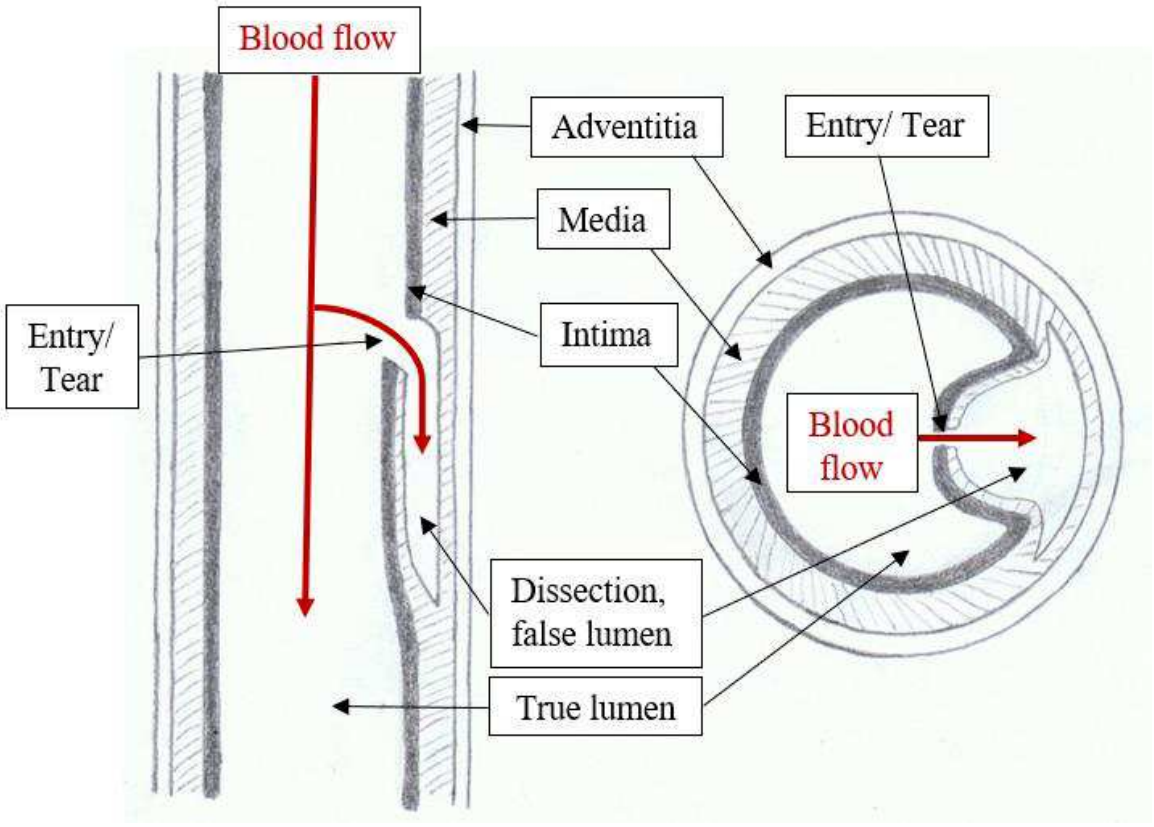

Figure 2: The dissection in the aortic wall seen in longitudinal cut (left) and cross-section (right), source: Author

5. Clinic

5.1 Most common symptoms

Most of the precursors mentioned above, including atherosclerosis, are symptom-free. Acute aortic dissection becomes symptomatic when the innermost layer of the aortic wall tears. This tear causes a sudden, very strong, sharp, ripping pain in the thorax, which is felt by more than three-quarters of patients with type A and above 60 percent with type B dissections [6]. Usually, this unbearable pain radiates to other body parts of the area, depending on the tear position. Radiation in the neck or back between the shoulder blades indicates mostly a thoracal dissection, while radiation of pain in the lower back or abdomen points to an abdominal dissection. Aortic branches can be obstructed not only from within due to the missing connection to blood flow but also from external pressure if the significant expansion of the aortic diameter compresses the branch from the outside. Colic pain in the periumbilical region can appear due to closure of the mesenterial vessels. Extension of the dissection in the longitudinal direction can also cause pain to move caudally. Hypotonia and tachycardia can either indicate active bleeding or be the consequence of major blood loss from the true lumen to the aortic wall or rupture. The major symptoms include acute aortic regurgitation and cardiac tamponade. Furthermore, massive pain, activation of aortic baroreceptors, obstruction of extracranial brain vessels, or cardiac tamponade can cause syncope in up to 20 percent of patients [17].

Approximately 20 percent of patients with aortic dissection present with irregular arterial pulses or even complete loss of them. The blood pressure in the extremities varies, showing a pressure difference between the extremities. A significant difference is typically correlated with ischemia in regions supplied by arteries branching off the aorta, which is indicative of poor prognosis [6].

5.2 Symptoms associated with Stanford type A dissections

Stanford Type A dissections that initiate in the ascending aorta or aortic arch are generally more severe and often more acute. This severity is attributed to the critical arteries branching off from this region, as depicted in Figure 3. If the dissection obstructs the coronary arteries, it can lead to myocardial ischaemia [18]. Complete closure leads to acute myocardial infarction. Dilatation or compromise of the aortic root can lead to incomplete valve closure, resulting in aortic regurgitation and acute heart failure. Apparently, this insufficiency of the aortic valve occurs in almost half of the patients suffering from type A

dissections. A common symptom is the acute new appearance of a diastolic heart murmur, sometimes with peripheral symptoms. Another heart disease caused by type A aortic dissection is cardiac tamponade. This tamponade is mostly visible in an X-ray and can lead to a Pulsus paradoxus, an extension of the jugular veins, and in worse cases to cardiogenic shock. In fact, pericardial tamponade is a serious complication of type A dissections, that most frequently leads to death [20]. In some aortic dissections, the Arteria carotis communis is cut off from the blood flow, which causes neurological failure or even ischemic stroke.

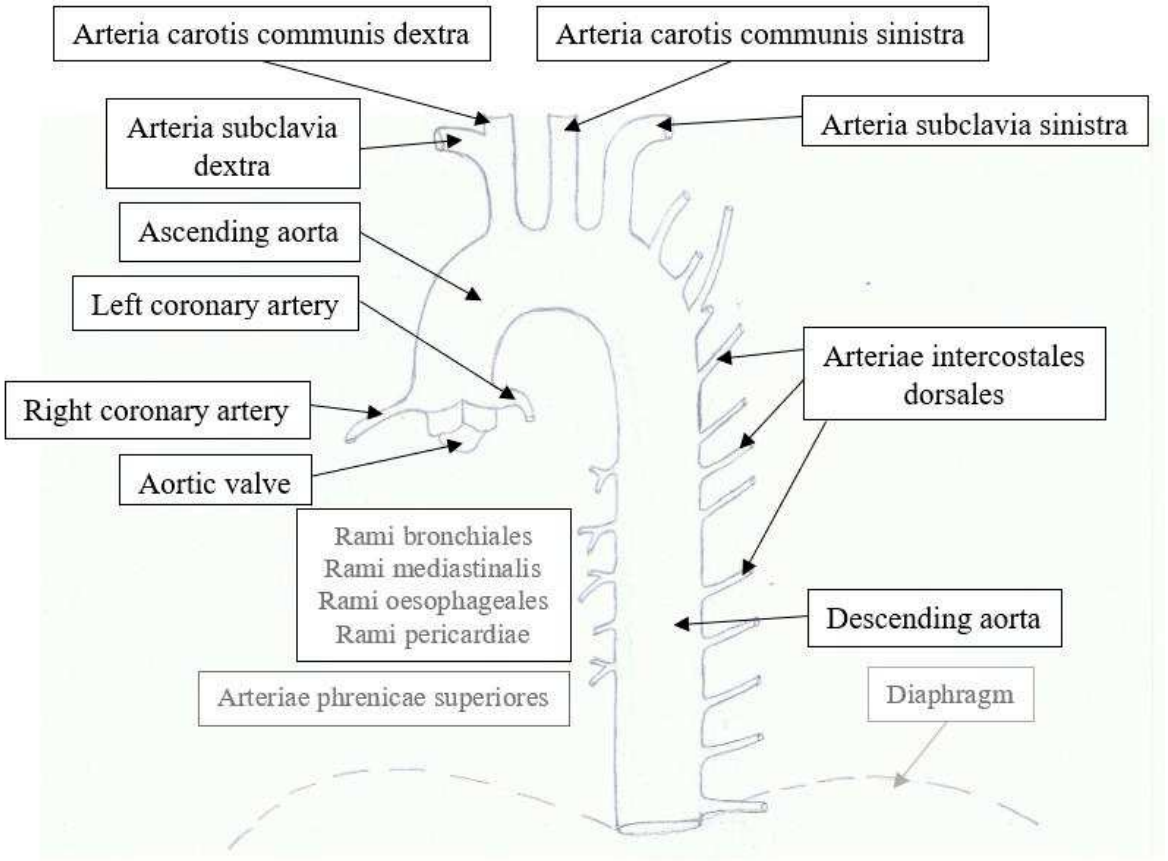

Figure 3: Thoracal aorta with its arteries branching off, Source: Author

5.3 Symptoms associated with dissection in the descending aorta

Stanford type A aortic dissection can extend further into the descending aorta, abdominal aorta, or even through its entire length. Therefore, the following symptoms and complications match both types A and B. In some cases, a pleural effusion can be observed in the X-Ray. This pleural effusion, with corresponding symptoms, can be a consequence of blood loss and inflammatory serous liquid, which can flow into the left pleura. Most other symptoms depend on the affected branches of the descending aorta, as shown in Figure 4 [18].

The Arteria radicularis magna, also known as the Adamkiewicz artery, is an artery branching off the aorta at approximately the ninth thoracic vertebra, supplying the spinal cord with blood. If its blood flow is cut off, symptoms of paraparesis or paralysis can occur [13].

Blockage of the right or left renal artery can impede proper kidney function. Symptoms such as flank pain, abdominal pain, fever, nausea, and vomiting may manifest in the event of complete obstruction of one or both arteries. Within the first 24 hours acute kidney failure or injury develops, becoming apparent in macrohematuria, oliguria, or anuria. Hypertension can be a consequence but is more likely in chronic ischemia of the kidney arteries [7].

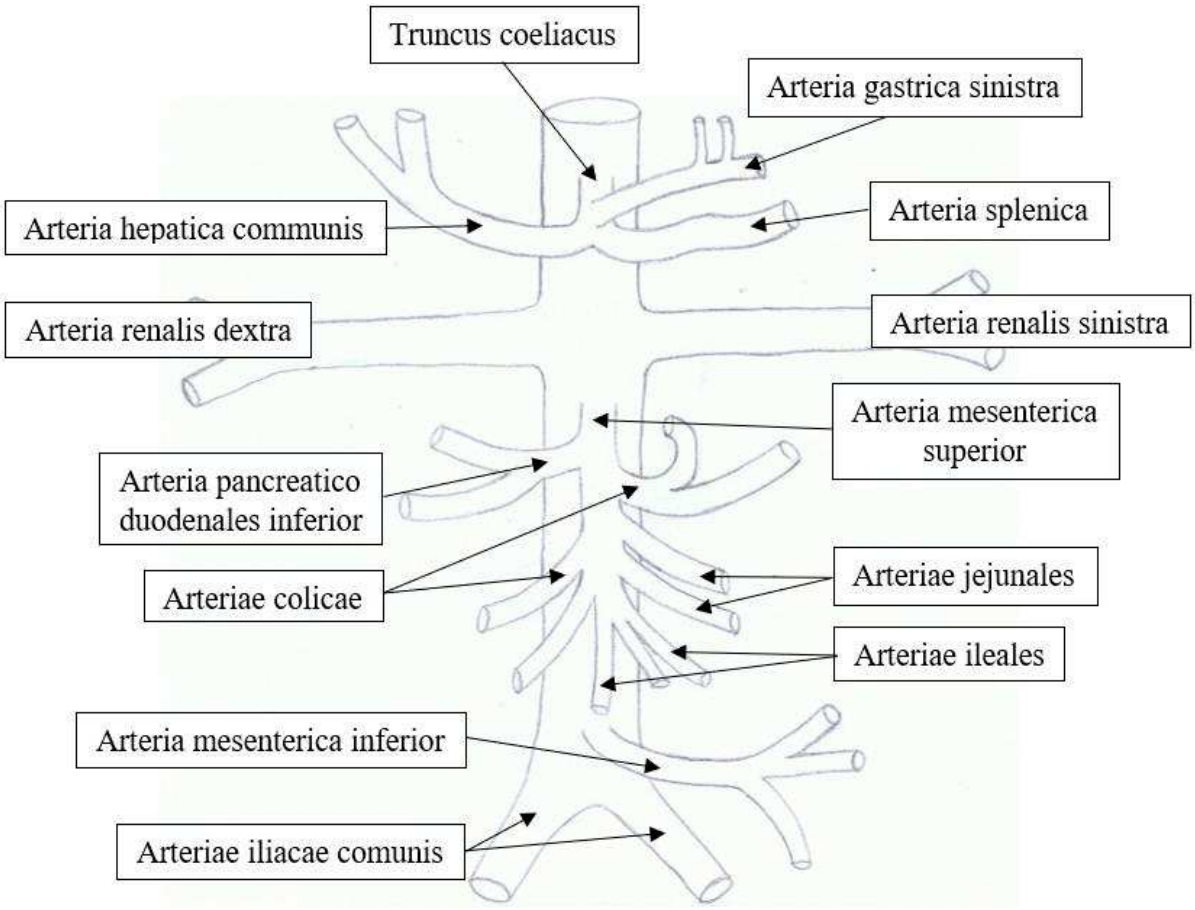

Figure 4: Abdominal aorta with its arteries branching off, source: Author

In cases of occlusion of an artery supplying one of the extremities, acute ischemia in the peripheral regions or neuropathies can appear. As seen in Figure 4, Truncus coeliacus (TC) provides oxygenated blood to the stomach, duodenum, spleen, and hepatobiliary system. The jejunum, Ileum, Colon ascendens, and descendens are supplied by the Arteria mesenterica superior (AMS). Furthermore, the Arteria mesenterica inferior supports the area between the colon transversum up until the rectum with blood. If one of the above arteries shows stenosis,

for example due to atherosclerosis, robust collaterals between these three arteries are slowly created. However, if blood flow is abruptly interrupted, as in the case of acute aortic dissection, there is insufficient time for the body to develop these collaterals. This scenario may have adverse effects on intestinal organs. Signs of occlusion of the celiac trunk or the superior or inferior mesenteric artery include an acute abdomen. In severe cases, blockage can result in intestinal infarctions [8]. Closure of the complete distal aorta, including the bifurcation aortae, leads to Leriche Syndrome, which includes acute or chronic ischemia in the regions of the arteriae iliacae communis. The acute symptoms of this syndrome are similar to those of peripheral arterial disease: pain, paleness, pulselessness, prostration, paralysis, and paresthesia. If the aortic dissection does not completely cut these two arteries, chronic symptoms such as claudication intermittens in the gluteal and thigh muscles, erective dysfunction, or micturition disturbances can develop [12].

The severity of the sequalae depends, but many of the symptoms mentioned above are complex and can lead to irreversible damage or if untreated even to death. An additional complication is the possibility of aortic rupture, causing serious amounts of blood to flow into the thorax, mediastinum, and/or abdomen. Acute bleeding quickly leads to hemorrhagic hypovolemic shock, making emergency surgery and reanimation inevitable. Symptoms in this case can be tachycardia with reduced systolic blood pressure, weak palpable pulses, paleness, sweating, thirstiness, and loss of consciousness. Radiologic signs of an impending perforation include a rapidly increasing diameter of the aorta and periaortic liquid [19].

6. Differential Diagnoses

Although the symptoms of aortic dissection can vary based on severity and whether arteries branching off the aorta are occluded, nearly all patients experience thoracic pain. Thoracic pain is a common symptom of various diseases that affect different organs. Therefore, before confirming the definitive diagnosis of aortic dissection, it is crucial to consider and rule out differential diagnoses. Medical history and physical examination can provide valuable information to identify the organ responsible for thoracic pain.

If pain depends on body position and movement, the cause is likely to be musculoskeletal. This is the most common cause and is occasionally associated with trauma, such as bruised ribs or costal sprains. In some cases, pain caused by aortic dissection radiates into the back. This type of pain can be misleading, as it closely resembles pain associated with a herniated disc [9].

Ordered by frequency, thoracic pain, depending on breathing, can be a sign of firstly pneumonia, then pulmonary embolism, and lastly pneumothorax. While pneumonia and pneumothorax can be seen in a thoracic X-ray, the diagnosis and recognition of pulmonary embolism involve a high Wells´- score, and preferably a CTA scan. Pulmonary embolism can sometimes show rapid and severe progression, too. Consequently, pulmonary embolism is considered one of the most critical differential diagnoses. If other symptoms such as coughing, B-symptoms, and the existence of risk factors such as smoking, age above 60 years, and male sex are present, malignancy could be possible and should be investigated [10].

If pulmonary causes can be excluded, thoracic pain is often attributed to the heart and its arteries. Typically, a patient with myocadiac infarction experiences sudden retrosternal, left-sided pain radiating into the left arm or jaw. Therefore, the symptoms are similar to aortic dissection. Chest pain accompanied by jaw pain, stress, coldness, or relief from rest is indicative of coronary heart disease and angina pectoris. When two or more of these symptoms are present, angina pectoris is highly likely. The cardiac origin of thoracic pain can usually be ruled out if only one or fewer of these symptoms are observed. Both coronary heart disease and myocardial infarction are more common than aortic dissection [10]. In cases of additional appearance of inflammatory symptoms, such as fever, feeling of illness, and elevated inflammation values, pneumonia or pericarditis are possible. If a cardiac cause is suspected, further specific diagnostic measures, such as echocardiography, coronary CTA imaging, ergometry, or myocardial scintigraphy, are required. An essential diagnostic measure involves assessing pulse and blood pressure in all four extremities, as variations in pulse strength may indicate aortic dissection. In contrast to myocardial infarction, where pulses typically remain uniform, in aortic dissection, the right subclavian pulse exhibits normal characteristics, whereas the remaining pulses are weakened or reduced.

Apart from cardiac or pulmonary causes, psychological issues, such as anxiety disorders, can lead to hyperventilation and chest pain. Through a thorough medical history and anamnesis, physiological causes can often be identified early on [9].

Lastly, gastrointestinal problems can lead to thoracic pain. These include gastroesophageal reflux, ulceration, rupture, and spasm of the esophagus. The pain associated with these conditions is frequently characterized by a burning sensation and may sometimes be accompanied by abdominal symptoms or difficulties in swallowing [10]. Furthermore,

dysfunction of the abdominal arteries leading to intestinal ischemia and its associated symptoms may manifest not only in aortic dissections, but also in conditions such as hernia or stenosis of the mesenteric arteries attributed to factors such as blood clotting disorders or atherosclerosis. Moreover, gastrointestinal chest pain may be influenced by factors such as the timing of meals, particularly late-night eating, and the composition of food, notably those with high fat content. Gastroesophageal reflux, for example, typically occurs after eating late before bedtime, after consuming high-fat meals, or after extended periods of fasting. Similar to the acute pain of the tear in the aortic wall in aortic dissections, tearing pain is experienced when the esophagus ruptures. However, the symptoms and causes differ from those of aortic dissection, facilitating differentiation.

7. Diagnostic

7.1 Physical Examination and Anamnesis

As in every case, physical examination and anamnesis is performed first. The ESC Pocket guidelines for aortic diseases 2014, in cooperation with the European Society of Cardiology [27], describe an aortic dissection risk score, the ADD-RS, to calculate the risk based on high-risk anamnesis, symptoms, and medical evidence. Nevertheless, every instance of acute type A dissection is considered a medical emergency, not allowing for an extended anamnesis and consistently categorizing it as a high-risk case.

The first category contains anamnestic high-risk factors, including Marfan- Syndrome and other diseases of the connecting tissue discussed above, as well as a positive family history of aortic diseases. Furthermore, a positive personal medical history of thoracic aneurysms, malfunction of the aortic valve, or previous operations or interventions in the area of the aorta belong to this category.

The second category describes high-risk symptoms, consisting of different characteristics of pain in the chest, back, and/or abdomen. Typical characteristics include abrupt onset of pain, high intensity, and a sensation of ripping or tearing pain. If one or more of these characteristics apply, this category is considered positive.

The last category of the score is medical evidence, indicating aortic dissection. In this category, physical examination, establishment of extended hemodynamic monitoring, continuous control of arterial blood pressure, pulse oximetry, vigilance, and neurologic status are essential. The category is considered positive if during examination one of the following malfunctions of the perfusion appear:

- Deficiency of pulses
- Pulsus paradoxus
- Difference of systolic blood pressure in between the sides or between upper and lower extremities
- Neurologic deficiencies

To measure and compare the pulses, the following Arteries should be investigated: A. carotis, A. subclavia, A. radialis, A. femoralis. Additionally, a diastolic murmur associated with aortic regurgitation can be discovered during auscultation. It is often described as a high-pitched, blowing sound with its punctum maximum above the left sternal border or the apex of the heart. Aortic regurgitation and hypotonia are also considered high-risk medical evidence [27].

Referring to Amboss's article about aortic dissection [19], the evaluation of ADD-RS is kept simple by adding one point for every positive category. This leads to a range of points between zero and three.

Patients with a type B aortic dissection with an ADD-RS of zero or one point, are considered as stable, showing a low or intermediate risk. Subsequently, further diagnostic measurements, such as the determination of D-dimer levels, are required. However, if the ADD-RS is greater than one, further diagnostic imaging, such as CTA, is needed.

An aortic dissection risk score of two or three points equals an unstable patient with a high risk of aortic dissection. Here, a distinction must be made between generally unstable and unstable patients with a high risk of aortic dissection. However, the first therapeutic measure is to stabilize the patient, regardless of the cause. A positive aortic dissection risk score should immediately lead to CTA to confirm or rule out aortic dissection. Additionally, in case of an unstable patient, it is recommended to consult a heart surgeon early on [19, 27].

7.2 Laboratory analysis

As mentioned above, measuring D-dimer levels can be useful, especially in cases of unclear clinical symptomatic presentation. However, it is important to note that D- Dimers are non-specific fission products of fibrin, indicating activation of coagulation. High levels can appear not only in many different diseases, such as pulmonary embolism or heart attacks, but also in pregnancy. Therefore, a positive test for D-dimers could be caused by aortic dissection but does not necessarily have to be affirmative. Further diagnostic testing is

required. However, if the test for D-dimers is negative, aortic dissection is very unlikely [11].

In addition to D-dimer testing, other laboratory analyses are required to evaluate the situation and detect complications. “Although there are no firmly established, clinically available serum biomarker tests that are specific for AD, there is considerable interest in developing biomarkers that may aid in early diagnosis or exclusion of AD.” [6 p5]. In cases of bleeding of the aorta, for example, anemia and slight leukocytosis can be found. In addition, CRP, procalcitonin, creatine kinase, Creatinine, Lactate, Glucose and Liver values, such as ALT and AST, should be taken. Furthermore, a high LDH value could be an unspecific sign for an involvement of the Tr. coeliacus or A. mesenterica branching off the aorta. To diagnostically separate an aortic dissection and a myocardial infarct, the amount of CK- MB and Troponin I and T in the serum are able to support the diagnostic. Both the CK-MB enzyme and cardiac troponin are signs of damage to the heart muscle, indicating myocardial infarction. However, myocardial ischemia or acute heart failure, and therefore elevated biomarkers, can also occur in acute aortic dissection [17]. If Marfan Syndrome is indicated, measuring circulating transforming growth factor-beta levels may be beneficial [6].

7.3 Electrocardiogram

Another, more specific diagnostic test to rule out the differential diagnosis of myocardial infarction is 12 channel Electrocardiogram (ECG). In comparison to the D-dimer test, an aortic dissection cannot be ruled out if the ECG appears normal, since there is no typical sign. In only 1-2 percent of the patients with aortic dissection ST-segment elevation appears [12]. While the range of abnormalities in the ECG of a patient with aortic dissection is wide, myocardial infarction or at least STEMI can be seen as an ECG abnormality. In addition, there is a rare possibility of acute inferior myocardial infarction caused by closure of the right coronary artery due to aortic dissection in this area. These patients experienced chest pain, and the ECG appeared abnormal. For this reason, an ECG might be useful for excluding a heart attack, given its rapid accessibility. However, it is not sufficient for ruling out the diagnosis of aortic dissection.

7.4 Computed tomography with Angiography

When angiography is performed concurrently with computed tomography (CT), it is referred to as CTA, standing for computed tomography with angiography (CTA). CTA is the method of choice and is considered the gold standard for diagnosing and monitoring aortic

dissection. CTA imaging is a highly effective and secure method, especially in acute situations where unstable patients require a quick and secure diagnosis. For combined angiography a contrast medium containing iodine is injected intravenously. Some patients show allergic reactions to contrast dye, and some patients may experience compromised renal function, rendering the use of contrast dye impractical [1]. Furthermore, it has the disadvantage of radiation exposure. However, in emergency situations and before every surgery or intervention, CTA must be performed regardless of radiation, and the disadvantages of contrast dye are negligible.

CTA appears to be a quick method with the possibility of viewing the entire length of the aorta, including most of its branches, allowing for the visualization of different layers and facilitating the creation of a 3D image of the vascular tree [47]. In the case of aortic dissection, it not only displays the two lumina and the membrane separating them but also enables the assessment of potential involvement of the branches. Additionally, other aortic diseases or precursors of aortic dissection, such as intramural hematoma or aortic ulceration, can be recognised [19].

7.5 Imaging Approaches for Aortic Dissections beyond CTA

- Chest X-Ray (radiography): There are signs of aortic dissection, which can be seen in an X-ray image of the thorax. These include widening of the mediastinum, left-sided pleural effusion, compression of the trachea, and/or a protrusion that marks the start of the dissection and entry into the false lumen. A false lumen, which is already further advanced, can be seen as a double outline of the aorta. However, owing to its sensitivity of 81 percent and specificity of 89%, it is not the most precise and secure diagnostic method [13]. Although chest radiography can be swiftly conducted in a stable patient with a low risk of aortic dissection, making it an easily accessible diagnostic test in most hospitals, radiography is of minor value in diagnosing aortic dissections and is therefore not part of the routine.
- Echocardiography: This medical imaging method uses ultrasound waves to create a cardiac image. A distinction must be made among transthoracic echocardiography, TTE, transesophageal echocardiography, and TEE. Both types of echocardiography have no radiation exposure and do not require contrast agents. In Echocardiography, the aortic valve and its function can be assessed, giving the possibility of recognizing aortic valve insufficiency or probable involvement of the valve in the dissection. Furthermore,

pericardial effusion can be observed or excluded [20]. Since assessment of the aortic arch is restricted in both variants, echocardiography is most useful in assessing the aortic root.

TTE is a non-invasive diagnostic imaging method used to not only examine the heart, but also the structures bordering the heart, such as the aortic root and ascending aorta. During this procedure, the patient lay slightly on the side, in a semi-supine position. An ultrasound transducer shows the heart and aortic root from different positions [47].

On the other hand, TEE is an invasive method that uses ultrasound waves. In this method, an endoscopic probe with an ultrasound transducer at its top is inserted in the esophagus dorsal to the patient's heart. In comparison to TTE, the transducer of TEE is much closer to the heart and aorta, and the image is not disturbed by artifacts such as ribs. Due to this advantage, the image extraction with low interference has a sensitivity of 97 to 99 percent, making it more specific than TTE images. The use of the motion mode can further improve the sensitivity by imaging the blood flow between the lumina and tears in the membrane [17]. Since aortic dissections mostly appear as an emergency, and patients are neither fasting nor stable, using TEE as a diagnostic method for aortic dissection might not be possible and is not part of the routine. However, it can be performed in intubated patients after the induction of anesthesia pre-, peri-, and postoperatively as an important method for visualizing the momentary state of the aorta, blood flow, and valve activity [58 p3].

- Magnetic resonance imaging with angiography: MRI can be combined with angiography (MRA) using contrast medium. In an MRA the entire aorta can be thoroughly visualized, ruling out aortic dissections or other aortic diseases. Contrast angiography proves most useful, allowing for observation. Additionally, it can be used to assess whether the aortic branches or the aortic valve are affected. In contrast to CTA, MRA avoids radiation exposure, but lacks the capability to depict calcifications within the aorta and other vessels. Visualization of calcifications enhances diagnostic clarity and contributes to more effective surgical strategy planning [27]. Even though MRA offers a sensitivity and specificity for aortic dissections of almost hundred percent, it is not suitable for emergencies, since the examination would consume an excessive amount of time [58]. Therefore, MRA is highly efficient as an imaging device for follow-up examinations, aimed at minimizing radiation exposure, but it is not suitable for acute settings.

8. Therapy

Considering the risk factors and causes, aortic dissection can in some cases be prevented by maintaining a healthy lifestyle. A healthy lifestyle includes a balanced diet, regular physical activity, and avoiding or quitting smoking cigarettes or abusing other drugs such as alcohol or amphetamines. While these adjustments may prevent the occurrence of aortic dissection, aortic dissection therapy involves the treatment of hypertension, symptom control, medical interventions, and surgical treatment.

The choice of treatment is contingent upon the type and severity of the dissection, as well as the patient's overall health status. Adjustments in lifestyle are recommended for every patient, but do not replace therapy. The main goals of treatment are preventing further dissection, reducing the risk of aortic rupture, and symptom relief.

8.1 Therapy of Stanford type A aortic dissections

Type A dissections involve the ascending aorta and, therefore, require emergency surgical treatment. Open surgery is typically used to repair these dissections, as it is associated with significant morbidity and mortality [14, 19]. However, the project part of this thesis predominantly centers on type B aortic dissections, placing significant emphasis on the role of medical imaging, particularly computed tomography angiography. Consequently, the discussion on the therapy of Type A dissections will be more succinct, with a primary focus on Stanford Type B dissections.

Surgical treatment is typically reserved for patients with aortic dissection type A, complicated or extensive aortic dissection. However, it is also indicated for patients who do not respond well to conservative management or are at a risk of complications. Acute Type A aortic dissection carries a 50% mortality rate within the initial 48 hours without surgical intervention. Despite advancements in surgical and anesthetic approaches, the perioperative mortality rate is 25%, with a notable 18% incidence of neurological complications [27]. While acute type A dissections should be treated as an emergency and require early surgical treatment, chronic type A dissections can be monitored and observed until surgery can be planned properly. Studies have shown that surgical results are the most promising if performed early and aggressively [40].

According to the 2019 ESC guidelines, surgical treatment is recommended for cases with high-risk anatomical features [27]. Predictors of complications are identified by:

1. Involvement of ascending aorta (Type A dissection)

2. Maximum aortic diameter greater or equal 50 mm
3. Progressive maximum aortic wall thickness: >11mm
4. Enlarging aortic diameter
5. Recurrent pleural effusion
6. Imaging-only detection of organ ischemia
7. Penetrating ulcer or ulcer-like projection secondary to localized dissections in the involved segment

The possibilities of surgical treatment of aortic dissections include open surgical-, endovascular-, or hybrid repair. The main aim of surgical intervention is to close the entry tear in the aortic wall to the false lumen and to secure the true lumen. Open surgical repair involves replacement of the entire aorta and damaged aortic branches [figure 7]. Typically, this approach is used in patients with Stanford type A dissection. There are currently no endovascular stent grafts approved for Type A dissections since their application in anatomically more complex regions, such as the aortic root or the aortic arch, is still very limited and technically demanding. However, some customized stent-graft designs or fenestrated grafts are available for use in patients with Type A dissection who have contraindications for open surgical repair [25, 42, 53]. The combination of open surgical and endovascular repair is called hybrid repair. An example is the frozen elephant trunk technique which combines prosthesis for the aortic arch and a stent-graft for the descending aorta on the distal side with a branched prosthesis for the arch vessels and ascending aorta on the proximal side [42, 53, figure 5].

Open surgery involves a large incision in the chest or abdomen and direct repair of the aorta. During open surgery, the affected section, or even the entire thoracic aorta, is replaced with a vascular prosthesis, as shown in figure 5. The replacement of the aortic valve can be performed simultaneously. The complexity of these procedures increases if multiple branches are affected and need to be reimplanted in the prosthesis, as in the aortic arch [53].

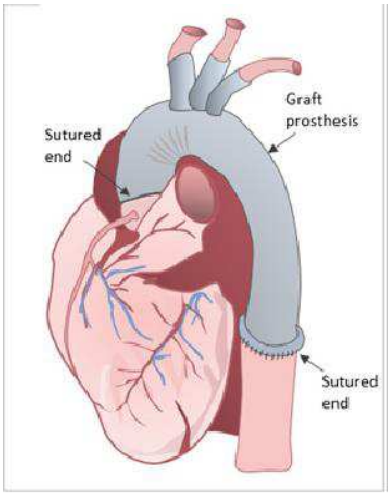

Figure 7: Total aortic arch replacement, source: [36]

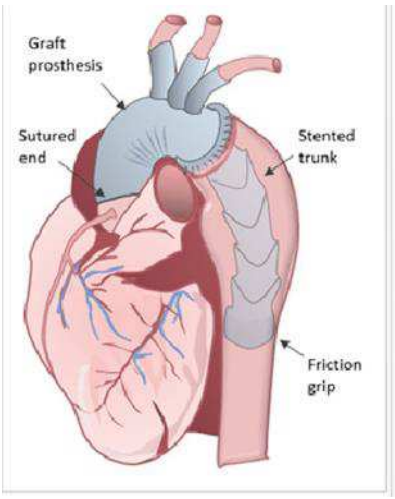

Figure 5: Frozen elephant trunk hybrid repair, source [36]

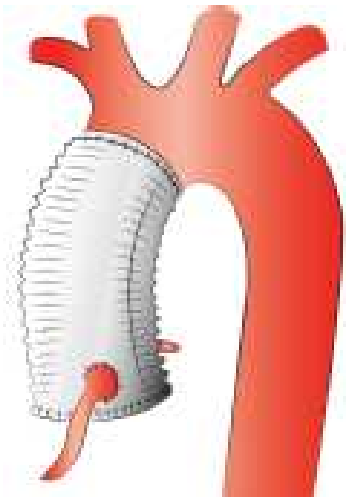

Figure 6: Bentall de Bono operation, source: [59]

Included in the options of open surgery are not only total aortic arch replacement [figure 7] but also various options to perform hemi-arch replacements [figures 5 and 6] up to the aortic arch. If annuloaortic ectasia or severe deficiency of the aortic valve is present, either the reconstruction of the native valve can be performed, or a valve/root replacement or the implantation of a valve-bearing conduit may be necessary and can be included in the surgery [24]. In the Bentall de Bono procedure [figure 6] the ascending aorta and aortic valve are replaced with either mechanical or biological valves. Valve-maintaining procedures include supracoronary hemiarch replacement and different types of David procedures. Hemiarch replacements can be extended to total arch replacements and with or without the hybrid 'Elephant Trunk' technique [figure 5].

According to ESC guidelines [27], it is advisable, whenever possible, to aim for replacement of the aortic root in cases where the dissection involves at least one sinus of Valsalva, as opposed to performing a supra-coronary ascending aorta replacement alone. The latter procedure is associated with subsequent dilation of the aortic sinuses, recurrence of aortic regurgitation, and necessitates a high-risk reoperation.

While non-aneurysmal, smaller, and localized tears in the arch can be repaired, the arch should be replaced in cases in which patients have an intimal tear within the aortic arch. If a replacement of the aortic arch is necessary, the distal end-to-end anastomosis between the prosthetic graft and the aorta is typically performed in zone 0 or 1 [figure 8]. This is often accomplished using the 'elephant trunk' approach. Replacement of the ascending aorta can be performed using a prosthesis with non-absorbable, possibly Teflon-reinforced materials [41].

Surgical intervention in cases of acute dissection is also the best option in the treatment of patients with Marfan syndrome or those who are not anatomically suitable for endovascular repair [14, 31].

8.2 Therapy for Stanford type B aortic dissections:

In contrast to highly lethal type A dissections, type B ADs can be separated into uncomplicated and complicated cases. Patients with uncomplicated, stable dissection are suitable for conservative therapy, including medication, blood pressure control, and observation. Patients with extensive type B dissection or complications, such as pleural hemorrhage, persistent hypertension, pain, and/or rapidly growing aortic diameter or length of dissection, are better treated with endovascular repair.

Complicated type B dissection is associated with a higher risk. Therefore, the AHA guideline 2021 [40] clarifies which type B dissections are classified as `complicated´:

1. Aortic rupture either free or contained: Hemothorax, increasing periaortic hematoma, mediastinal hematoma or a combination of the named
2. Branch artery occlusion and malperfusion with or without clinical evidence of ischemia
3. Extension of dissection flap either distally or proximally (retrograde dissection)
4. Progressive aortic enlargement of the true, false or both lumens
5. Intractable pain or uncontrolled hypertension [34]

8.2.1 Conservative Treatment

As explained above, the indications for conservative therapy of aortic dissections are Stanford type B dissections without high-risk anatomical features or complications. The symptomatology is rather mild or can be missing completely [19]. However, it is imperative to emphasize that these are indications for patients to receive only conservative treatment. Considering this, conservative measures are a crucial addition to other treatments. Observation and reduction of arterial blood pressure are essential for every patient diagnosed with aortic dissection. As known from experience with patients with uncomplicated type B aortic dissections, who benefit from conservative treatment, the prediction of the progression of false lumen thrombosis and aortic remodeling in the long term is crucial [31].

As the majority of patients with acute aortic dissection are hemodynamically unstable and in pain, the first-line treatment is pain medication. Opioids, especially morphine, are used to

achieve analgesia. Additionally, a preferably large-bore peripheral intravenous line should be applied. Depending on the patient's condition, type of dissection, and individual situation, intravenous fluids or blood can be supplied more efficient [14].

The initial therapy is strict control of blood pressure and heart rate, reducing the pressure to a target value of < 130/80 mmHg and a heart rate of less than 60 beats per minute. During treatment, blood pressure should be closely monitored and maintained at a level appropriate for each individual patient. Different variations of medications are effective to achieve this target value, or reducing it as long as an adequate cerebral, coronal and renal blood circulation is ensured. The antihypertensive medications of choice are beta-blockers with the additional use of diuretics or vasodilators like ACE- inhibitors or calcium antagonists. The options of an acute intervention with beta-blockers are dosing Metoprolol 5 mg i.v. up to four doses at intervals of 15 minutes, Esmolol 50 to 200 µg/kg/minute in a constant intravenous infusion, or Labetalol 1–2 mg/minute in a constant intravenous infusion. Another option is an initial bolus of 5–20 mg with additional doses of 20–40 mg every 10–20 minutes until either blood pressure control is achieved, or a total dose of 300 mg has been administered. Subsequently, additional 20–40 mg doses can be given every 4–8 hours, as needed. As a calcium antagonist Verapamil 0,05–0,1 mg/kg as a bolus or Diltiazem 0,25 mg/kg as a bolus or 5–10 mg per hour as a constant infusion can be administered [14, 39].

If the systolic blood pressure remains high despite the use of beta-blockers, Nitroprusside can be initiated in a constant intravenous infusion at 0.2–0.3 mcg/kg/min and titrated upwards as needed to control blood pressure. Nitroprusside should not be administered without beta-blockers or calcium antagonists since reflex sympathetic activation in response to vasodilation can increase ventricular inotropy and aortic shear stress [14].

While almost every combination of antihypertensives is acceptable, antihypertensive medications primarily exhibiting vasodilatory effects should be approached with caution and avoided. Examples include Hydralazine or Minoxidil, as well as beta-blockers with intrinsic sympathomimetic activity (ISA), such as Acebutolol or Pindolol. Reducing the arterial blood pressure and the force of the heartbeat can help decrease the shear forces acting on the aortic wall and reduce the risk of further tearing. It can prevent organ damage and improve aortic wall integrity [39, 38].

As mentioned above, observation is another important aspect of conservative treatment for aortic dissection. Signs of worsening symptoms or new complications, such as organ

dysfunction, aortic rupture, or aneurysm formation, should be considered and therefore looked out for. Imaging studies such as CTA scans or MRI should be performed regularly to monitor and assess possible disease progression of the dissection and to determine the need for surgical intervention [31]. Heavy physical activity and exertion are not recommended in most cases. Without surgical intervention, CTA is usually performed before discharge, followed by an update after six months, one year, and continuously yearly, depending on the changes and severity. A similar guideline for post-surgery CTA control scans exists, monitoring the aorta for the rest of the patient's life, as the weakened aorta may develop a redissection or aneurysmatic degeneration above or below the surgically restored part [17, 38].

While observation, pain control, and reducing blood pressure and heart rate are the most important aspects of the initial treatment of acute aortic dissection, other measures can be secondary, but necessary. Secondary treatments include, in addition to the lifestyle changes mentioned above, the consistent discontinuance of existing diabetes mellitus and dyslipidemia. Since hyperglycemia and high levels of LDL-cholesterol can damage vessels, regulating these values can prevent further damage to the already weakened aorta and other vessels.

8.2.2 Treatment options of complicates cases

Complicated type B dissections and dissections with high-risk anatomic features are indications for surgical treatment or intervention. Minimally invasive thoracic endovascular aortic repair (TEVAR) is the preferred worldwide standard for reducing morbidity and mortality. Although type B aortic dissections are mainly treated conservatively, surgery is also indicated for patients who do not respond well to conservative management or are at risk for complications. The main surgical approach for aortic dissection type B is endovascular repair with TEVAR [figure 9].

Preoperative Management

Prior to surgery, the patient may need to undergo further testing, such as CTA, or other imaging methods, such as MRA, to assess the extent of the dissection and prepare the procedure. As explained in the diagnostic section, adding angiography to imaging methods is mandatory. While the scan is used to confirm the diagnosis of aortic dissection and determine the best approach for the procedure, it is nonetheless a case-by-case decision based on individual pathology, anatomy, and the patients' medical history. Patients should

also receive preoperative medication to reduce the risk of complications during surgery. In addition, patients should be closely monitored for changes in their condition [14].

Endovascular Surgery

As a safe and effective alternative to open surgery procedures and mainly used in type B aortic dissections, endovascular stent graft implantation can be performed to treat aortic dissection. Thoracic endovascular aortic repair is a less invasive approach that involves the use of a stent graft to reinforce the aortic wall and prevent further tearing and late complications by initiating the aortic remodeling processes. The procedure involves sealing the proximal intimal tear through implantation of a membrane-covered stent graft, redirecting blood flow to the true lumen, and thereby enhancing distal perfusion. Thrombosis of the false lumen leads to its shrinkage, thereby preventing aneurysmal degeneration and ultimately mitigating the risk of rupture over time. TEVAR has been shown to be associated with less blood loss and shorter recovery times. However, it is not suitable for all patients, and open surgery may be required in some cases [32, figure 9]. Before the procedure, it is important to evaluate the degree to which the paired intercostal arteries are covered, as excessive coverage could lead to paraplegia caused by reduced blood supply to the spinal cord.

Dacron stent grafts are most commonly used. These grafts typically consist of a Dacron tube attached to a metal framework constructed from nickel and titanium, which possesses a temperature-dependent alloy with shape memory properties. Owing to the components of stent grafts, they have the capability to compress into a diameter of less than one centimeter and can subsequently be deployed and expanded at a specific location within the aorta or target vessel [53].

Stent grafts can be categorized into exoskeleton and endoskeleton types based on their structural design. While exoskeleton stents have an external metal framework that provides support from the outside, endoskeleton stents have an internal metal framework. The choice between these designs depends on the specific clinical requirements and anatomical considerations.

In cases where the dissection involves important branch vessels, such as the renal arteries, fenestrated stent grafts are designed with openings (fenestrations) to accommodate the branches of major vessels. The optimal length, timing, and percentage of aortic diameter oversizing, resulting in different wall tensions, are crucial factors for successful treatment.

For the descending aorta the insertion of stent-grafts is considered the treatment of choice [25, 42, 53]

TEVAR is a minimally invasive procedure. In cases with progression of the dissection, especially in cases with growing distal aortic diameters or endoleaks, TEVAR can also be performed as a second- or third-stage procedure [32]. A broad spectrum of differently designed TEVAR devices exists, since they are also applicable for aortic aneurysms, aortic transections after blunt chest trauma, penetrating aortic ulcerations, or intramural hematoma. For perioperative planning and to be able to choose the individually fitting stent graft, the data of the aortic geometries of the false and true lumen, including their biomechanical properties and the characteristics of entries and re-entries, are important. Additionally, the topography of the proximal landing zone [figure 8] should be known. In the context of aortic interventions, the landing zone refers to the segment of the aorta where an endovascular device, such as a stent graft, is positioned to secure proper fixation and sealing. In numerous instances, when the vertebral artery is well balanced and not hypoplastic on the right side, the left subclavian artery is overstented [33].

TEVAR involves several steps:

1. Access: During the procedure, a stent graft is inserted into the thoracic aorta through a small incision in the groin. If necessary, preemptive cerebrospinal fluid drainage is recommended for patients at a high risk of spinal ischemia.

2. Deployment of the stent graft: Once the catheter is placed in the femoral artery, it subsequently advances under fluoroscopic imaging and X-ray guidance to the dissection site. The stent graft is then positioned to cover the tear area. There should be an adequate 'landing zone' in the proximal and distal regions of the graft that is approximately 2 cm in length. As soon as the catheter is in place, the stent graft is deployed across the dissection, reinforcing the aortic wall, and sealing off the false lumen. The stent graft is designed to conform to the natural curvature of the aorta and prevent further tearing [41, 37].

3. Completion angiography: Once the stent graft is in place, completion angiography is performed to confirm that the stent is correctly positioned and the blood flow in the aorta is restored.

4. Postoperative monitoring: The material of the stent, when pressed against the vessel walls, becomes covered by endothelium, a process known as endothelialization, which helps maintaining the biocompatibility of the grafted segment. As long as endothelialization is incomplete, dual antiplatelet therapy with aspirin and clopidogrel is necessary for a certain period of 6 to 12 months to prevent early thrombotic closure in the case of an intracoronary stent [43]. Further postoperative treatment and monitoring applies to all surgically treated patients, as explained below.

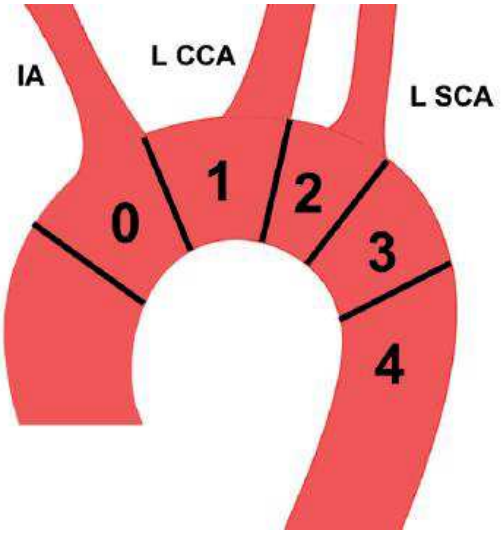

Figure 8: Landing zones of the aorta, IA: innominate artery, LCCA: left common carotid artery, LSCA: left subclavian artery, source [45]

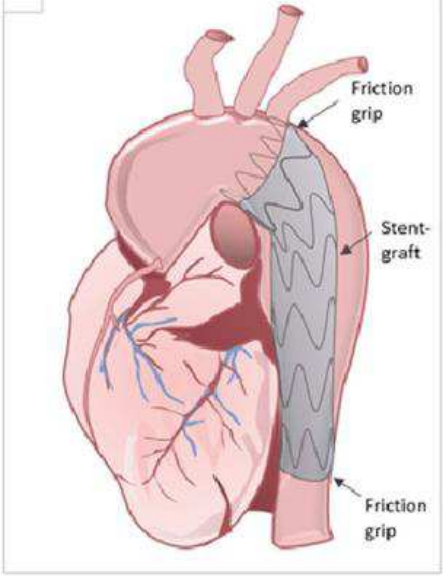

Figure 9: Endovascular Repair, TEVAR, source: [36]

8.3 Postoperative Management and Complications

After the procedure, patients are closely monitored in the intensive care unit for any signs of complications, such as bleeding, infection, or stent graft migration. Follow-up imaging studies are performed regularly to assess the status of aortic repair and monitor for new complications [44].

Possible complications of aortic dissection surgery, regardless of the type of procedure, may affect several organs. Apart from general complications of surgical treatment, such as postoperative bleeding or infection, other procedure-related pathologies can appear that possibly lead to death. This includes ischemic events, such as stroke due to embolism, neurological deficiencies, myocardial infarction, and kidney failure, especially if the dissection involves the renal arteries. The most important late-onset complications are re-dissection, the development of localized aneurysms in the weakened aorta, and progressive aortic valve insufficiency. These complications may necessitate surgical or endovascular

intervention. Other complications include damage to the surrounding organs, increased risk of blood clots, and arrhythmias [40, 43].

There are procedure-related risks concerning TEVARs, such as the risk of inadequate proximal or distal landing zones due to extremely dilated aortic diameters, high degrees of tortuosity as in kinked aortas, or unplanned left subclavian artery coverage. In some cases, with short proximal landing zones, adjunctive aortic debranching procedures with different surgical debranching options may be required. Further procedure-related risks with TEVAR include stent collapse, aortic perforation, especially on the proximal side, bird beaking, migration of the stent, device failure itself, or even rupture of the graft. Generally, the degree of calcification of the entire aorta, as well as the access vessel anatomy, is essential. Especially in cases with small peripheral diameters or heavily calcified femoral arteries, the risk of complications is elevated [44].

Furthermore, leakage of blood into the aneurysm sac, a condition known as an endoleak, may occur. These endoleaks can be classified as I-V according to the AHA Guidelines 2021, as follows [40]:

Type Ia: Leakage in the area of the proximal attachment site

Type Ib: Leakage in the area of the distal attachment site

Type II: Retrograde blood flow into the aneurysm sac through one (IIa) or multiple (IIb) side vessels

Type III: Leakage due to mechanical failure of the stent graft resulting from separation of modular components (IIIa), as well as fractures or holes in the endograft (IIIb)

Type IV: Leakage due to graft coverage in the sense of graft porosity

Type V: Aneurysm expansion without a visible leak in imaging, possibly due to endotension

Despite technical advancements, the mortality rate has ranged from 7% to 36%. Predictors of poor outcomes include hypotension, renal failure, age > 70 years, sudden onset of chest pain, pulse deficit, and ST-segment elevation on ECG [40].

Part II: Project

9. Introduction

Transitioning from the theoretical framework displaying the complex disease of aortic dissections, encompassing causative factors, clinical presentations, diagnostic methodologies, and therapeutic modalities, the focus will now shift towards the practical part. In context of this thesis, the pioneering project is centered on the conversion and segmentation of CTA scans capturing Stanford type B aortic dissections. The theoretical background, discussed earlier, forms the medical basis of this project.

In the ensuing exploration, the emphasis lies on the intersection between theoretical understanding and the implementation of advanced medical imaging and computational analysis. The project presentation of technology-driven image processing and segmentation with the overarching goal of refining diagnostic precision and therapeutic approaches.

In recent years, the integration of algorithmic software and advanced imaging techniques for procedural planning has become increasingly important, as three-dimensional (3D) imaging techniques allow for more precise and detailed visualization of the aortic anatomy. Subsequently, it enables more precise and prompt diagnoses, while also facilitating the planning of surgical interventions. Especially in the planning of complex procedures for individuals with aortic conditions such as Stanford type B aortic dissection, a quick and accurate visual assessment plays a critical role in clinical decision making [29, 52, 55].

The second part of this thesis aims to investigate the use of 3D imaging techniques in the diagnosis and management of type B aortic dissections. Specifically, this thesis focuses on the collection of 40 cases, the process of converting CTA scans into an anonymous format, and analyzing it in the open-source software “3DSlicer” by the segmentation of type B aortic dissections, including both the true and false lumen. This process concludes with a description of the 16 cases segmented by the author.

By exploring different open-source software programs for segmentation and various segmentation methods, the final goal of successfully segmenting the CTA scans was achieved. Furthermore, these, in total 40, segmentations of type B aortic dissections will be used to create a “ground– truth” dataset of segmented aortic images. After publishing the database, future projects may use them to for training and assessing algorithms. To develop an artificial intelligence (AI) program capable of performing automated segmentation, a database containing a “ground truth” dataset is mandatory. While the semi-automatic

segmentation process was proven to be rather time-consuming, an automatic segmentation program could allow the same advantages and improvements in decision-making and therapy for patients with aortic dissection, but within a shorter timeframe [52].

10. Material and Methods:

10.1 Patient Selection, Data Extraction and Conversion

Initially, the Department of Radiology of the Medical University of Graz forwarded the first list of documented patients diagnosed with Stanford type B aortic dissections, with a short description of the case. Subsequently, the patients on the list and the corresponding CTA scans underwent a thorough examination to identify 40 cases of clear type B dissection with high-quality CTA scans.

The study connected to this thesis was approved by the ethics committee of the Medical University of Graz (MUG), Austria (EK-34-161 ex 21/22, Medical University of Graz, Austria). All patient-specific data has been removed during conversion from DICOM to Nearly Raw Raster Data (NRRD) format. The head and facial regions were cropped from the CTA files; hence, informed consent was not required for this retrospective study [Appendix].

During retrospective recruitment, the dissections were separated by surgeons into uncomplicated and complicated type B ADs by manually reviewing the CTAs. Since artifacts and complexity of the involved structures in CTA scans of aortic dissections could cause complications during the segmentation process, CTAs with excessive artifacts due to metal implants, such as patients after TEVAR or CTA scans with significant motion artifacts, were ruled out. However, motion artifacts of the intimal flap cannot be completely avoided and are therefore seen in some or most CTA scans [53]. Additionally, CTA scans with clear contrast between the true and false lumen were preferred. Some of the suitable, operated type A dissections, which show a postoperative type B dissection, were systematically marked for backup purposes for future follow-up studies.

All CTA data were acquired during routine clinical practice. Therefore, the selected routine CTAs were not ECG-gated. Only medical CTA scanners were used, which are qualified medical products and therefore must routinely undergo maintenance and quality control under the responsibility of a qualified medical physicist [17].

The segmentation group visually checked the collected CTA images to confirm the diagnosis. Following the assessment, the pertinent data was extracted as Digital Imaging and Communications in Medicine (DICOM) from the local hospital network- and seamlessly integrated into the program "3D Slicer."

"3D Slicer" is a free and open-source software package for image analysis and scientific visualization. It is compiled for use on multiple computing platforms, including Windows, Linux, and MacOS, and is used in a variety of medical applications, including different types of cancer and cardiovascular diseases. The software provides image registration, handling of DICOM images, manual editing, automatic image segmentation, and other capabilities. This includes interactive visualization of volumetric voxel images, polygonal meshes, and volume renderings. Furthermore, it supports a rich set of annotation features such as measurement widgets or customized color maps [48].

As seen in figure 10-12 page 46, CTA scans can be uploaded, opened in various formats, and viewed in four windows, each representing the scan in one of the planes. Specifically, there was a window in the sagittal, transverse, and frontal planes. The fourth window displays comprehensive results of the current activity. For instance, this could include the product of the segmentation process or the box remaining after cropping.

Subsequently, the DICOM data information was converted into an anonymized format, wherein any identifiable details, including scans of the head, were systematically removed. This designated format was the NRRD format chosen for its efficacy, aligning with privacy and confidentiality standards. In the following, extraction and conversion are explained step-by-step.

1. One of the selected CTA scans were opened in the network "openMEDOCS"
2. To extract to scan in DICOM format, "Untersuchung" had to be selected, followed by "kopieren", then "Ok"
3. Subsequently the extracted DICOM CTA scans were filed and numerical designated from 1 to 40
4. The program "3D Slicer" was opened
5. To upload the CTA scan, "file" was selected, then the file with the chosen DICOM data was selected and the button "load" was clicked
6. If the scan included the head of the patient, the data were cut to guarantee anonymization. To do so, the module "volume rendering" was selected, followed

by enabling “crop” by ticking the box and displaying the ROI by opening the eye, as shown in figure 10. The CTA scan could now be precisely delineated in all three planes (sagittal, frontal, and transverse) using the crosshair, ensuring that the head and neck of the patient are severed at the shoulder level. Figure 12 shows the sizing handles in all planes in the 4-window view.

7. Next, “Crop volume” had to be selected. The input volume “input ROI” = “Volume rendering ROI” was selected. As an output volume the name “CTAx” was picked with `x´ standing for the applied number 1 to 40. To finalize cropping, the button “Apply” had to be clicked.
8. To save the result “Save data” must be selected. As options for possible data formats appear, only the file in the NRRD format should be selected and saved, as shown in figure 11.

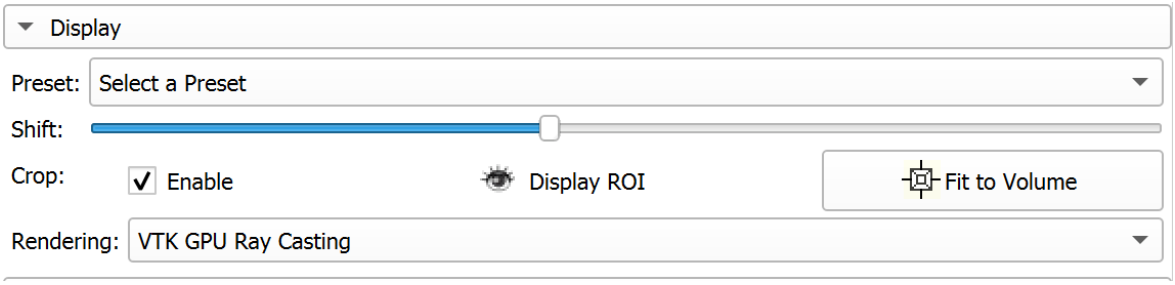

Figure 10: Screenshot of the module “volume rendering” in the program “3D Slicer”. Settings for cropping the volume, source: Screenshot from “3DSlicer” by author

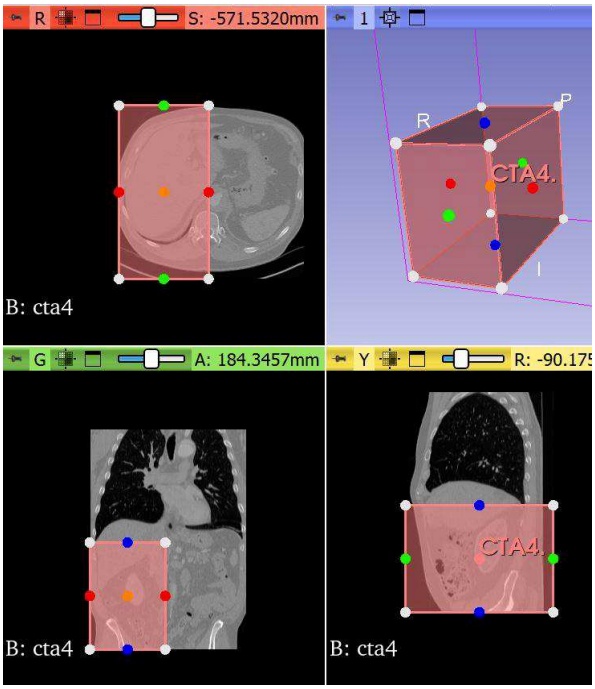

Figure 12: 4 window view of the cropping module source: Screenshot from “3DSlicer” by author

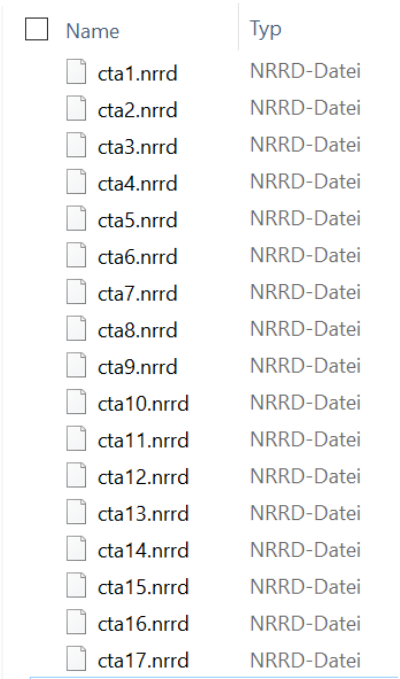

Figure 11: File with the list of CTA scans in NRRD format in the program “3D Slicer” source: Screenshot from “3DSlicer” by author

10.2 Segmentation

In the next step, segmentation of each CTA scan was started. Manual segmentation is a time-consuming process that requires highly specific knowledge of the anatomic and radiologic properties of CTA scans, as well as proficiency with suitable software tools. Available software tools often provide semi-automatic functions to accelerate and simplify the segmentation process [53]. For this process, the author initially became familiar with segmentation software. The process from the NRRD CTA data to the final segmentations involved multiple attempts, as handling the originally chosen program proved significantly more complex and encountered several issues. Subsequently, it was necessary to start anew by choosing and learning another segmentation program, which in turn consumed additional time.

10.2.1 Segmentation process with “SimVascular”:

The initial attempt involved utilizing the program “SimVascular” for segmentation. “SimVascular” is an open-source software, whose primary software system is descended from the ASPIRE2 internal lab software. It was designed by Ken Wang and Nathan Wilson and is customized for building geometric models from medical imaging data, generating the data files needed to run flow simulations, and processing and visualizing the results from these simulations. Additionally, it can be used to interact with and visualize medical imaging data, directly providing insights into vascular disease processes.

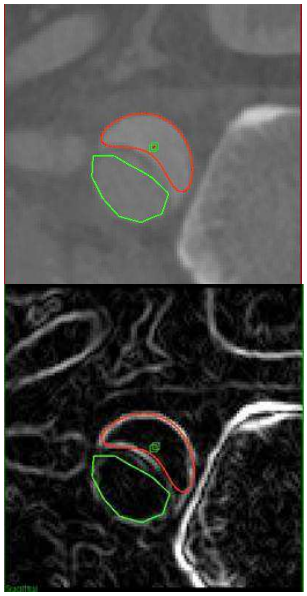

Figure 14: Outlines of the true (green) and false (red) lumen in one layer in horizontal plane, source: Screenshot from “SimVascular” by author

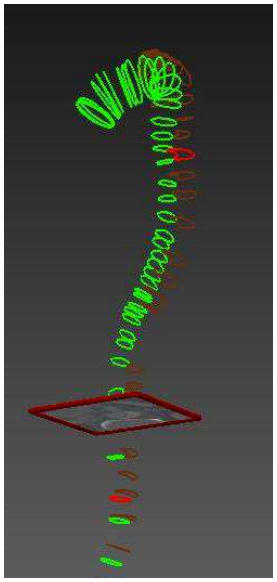

Figure 15: View showing outlines of true (green) and false (red) lumen in layers through the course of dissections, source: screenshot from “SimVascular” by Author

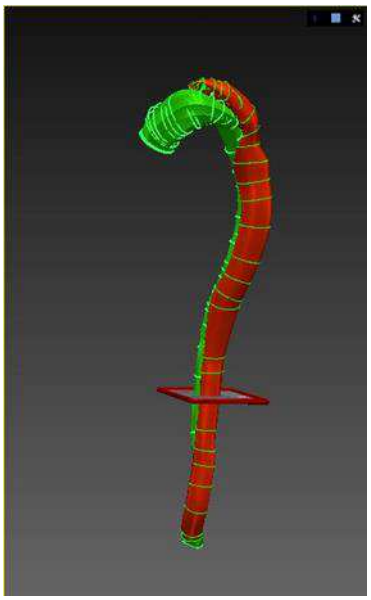

Figure 13: Completed segmentation of the aortic dissection with true (green) and false (red) lumen, source: screenshot “SimVascular” by author

Subsequently the idea is to aid vascular surgeons in treatment planning, as well as to help engineers in designing better medical devices.

The sequential segmentation process is described as follows:

1. First, the software had to be installed and opened
2. Secondly, a SV Project had to be created by clicking “file”, then selecting “create SV project” and subsequently putting in a name such as “CTAx” in our case. `x` standing for the assigned number of the CTA scan.
3. To open the CTA file “file”, then “open file” was clicked. Thus, a CTA scan in the correct NRRD format can now be selected.
4. In preparation for the segmentation, first, a path through each true and false lumen of the dissection had to be created. For this “path”, then “create path” was selected. Subsequently, a name for the path, such as “true lumen”, was added.
5. To start the designated path, its name is clicked. Within the CTA scan, a crosshair becomes visible, serving as a tool to precisely designate the desired lumen by clicking on its center. This action effectively marks the lumen across all three planes. Upon confirming the selection, the "Add" function was invoked to record the chosen point. The subsequent step involves navigating through the entire dissection, systematically marking the lumina at intervals of 5 to 10 layers, depending on the complexity of the region. A list of coordinates of the fixed points in the CTA scan appeared, enabling editing in the future.
6. By left-clicking the name of the path, “point 2D” , then “size” can be selected. The size of the points should be adjusted, as required. However, for most CTA scans, a size of 2 or 3 was sufficient.
7. The module “Segmentation” was clicked on to start the segmentation for one of the dissection lumina. Subsequently “Create contour group”, then “path selecting” should be selected. Confirmation was given by clicking “OK”.
8. The size of the selected area following the path can be set using a double click on the name of the path. In most cases a size of 60 to 80 was sufficient.
9. The targeted lumen was outlined by selecting the "polygon" tool. Upon activation, the tool manifests as a small-polygon cursor on the CTA scan. The lumen was marked by strategically placing up to 10 polygons, outlining it. To conclude the outlining process, a double click is utilized to place the final polygon. Subsequently, the "smooth" option was chosen to refine the outline by rendering it

more rounded and fitting. Figures 14 and 15 show the horizontal and 3D outlines, respectively.

10. While navigating through the entire dissection, Step 9 is repeated in every fifth layer, systematically segmenting the targeted lumen.
11. To be able to view the 3D segmentation as a preview, “lofting preview” should be enabled after completing the outlines of the targeted lumen. Subsequently, the preview is checked for overlaps, missing segmentation parts, and segmentation errors. Overlapping layers, for example, in curvatures or deriving branches, and single layers must be deleted. Bends and edges in the segmentation had to be checked for correctness by comparing it with the original CTA scan.
12. After correcting and completing the segmentation of one lumen, steps 4 to 11 were repeated for the other lumen.
13. If both lumina are segmented, align together and match the CTA scan, the completed Segmentation, as seen in figure 13, was saved by clicking “Save” and naming it “CTAxs” with `x´ standing for the assigned number and `s´ for segmenting.

After the initial segmentation of the first five CTA scans, the segmentation method and the program “SimVascular” was disseminated and elucidated to the remaining medical team members, before proceeding with the remaining scans. Senior team members evaluated the completed segmentations for medical correctness. Certain difficulties arose during the segmentation process using “SimVascular.” The following problems will be explained in more detail in the Discussion section:

Segmentation inaccuracies arose from overlapping issues in outlining lumina, notably in the aortic arch and curvatures, resulting in drastic layer reductions. Automatic gap filling by the program leads to further inaccuracies, especially in the aortic arch. Other problems leading to inaccuracy were difficulties in editing outlines, challenges while segmenting aortic vascular branches owing to numerous overlaps at the branching points, and sporadic software errors leading to missing parts of the aorta in the segmentation view. Furthermore, segmentation using “SimVascular” was very time-consuming. Subsequent editing, correcting, and rectifying errors proved to be demanding, with certain CTA scans requiring several additional hours.

To use segmentations in the future, it is crucial to medically align the segmentations with the original CTA data and to employ standardized methods or schemes. This involves

defining ground rules, such as having fixed starting and endpoints for segmentation, as well as maintaining a consistent distance between manually segmented layers. The lack of this targeted accuracy, the impossibility of the ground rules to be implemented, and the cumulative challenges mentioned, prompted the team to decide against further pursuing segmentations using the program “SimVascular”.

10.2.2 Segmentation Process with 3D Slicer

It is one of the aims of this segmentation project to create a “ground truth dataset” of aortic dissections, which can serve as a basis of future projects and as teaching data for artificial intelligence (AI) models. To achieve high-quality segmentations that comply with expectations, further reviewing and consulting meetings with the technicians were held. As a result, it was agreed on using the software “3D Slicer”, which has already been used for the conversion of the data.

Learning the segmentation process with “3D Slicer” showed the advantage that a valued member of the technician team, Antonio Pepe [52], had already used the segmentation tools and even performed a tutorial video. After successful segmentation of the first five CTA scans and evaluation of the quality and accuracy, the remaining 35 CTA scans were divided among the segmentation group. The segmentation team consisted of three cardiac surgery residents and one medical student, the author.

Even though all members worked with the same program “3D Slicer”, various semi-automatic methods of creating segmentations were performed and compared. Despite the differences in the creation of 3D segmentation, ground rules were set for the entire team.

1. Starting point of the segmentation at the aortic valve area
2. Ending point in the proximal part of the femoral arteries
3. Vascular branches in the aortic arch, as well as the mesenteric, renal, and femoral arteries, were segmented, including the origin and subsequent centimeters of the branches. Thus, better visualization of the extent of dissection was enabled.
4. Separate segmentations for true lumen colored in “mass green” and false lumen colored in “artery red” were created
5. If a luminal thrombus was markedly visible, it was segmented as a third lumen colored in “thrombus red”

The general segmentation process from the NRRD-format CTA scan to the completed segmentation is described below.

As preparation, the software “3D Slicer” had to be opened, and additional tools for segmentations were installed. This is achieved by accessing the "View" option, selecting "Extension Manager," then "Segment Editor," and choosing "ExtraEffects" for installation. To enable these effects, the program had to be restarted.

To start the segmentation process, a CTA scan of aortic dissection was loaded into the software by selecting "Files," choosing "Add files," and subsequently selecting the targeted CTA scan in NRRD format. To remove noise while preserving the edges of the images [54], iterations were set up by selecting "Search," followed by "Curvature Anisotropic Diffusion." The iterations should be set to 7, with the input volume as “CTAx” and the output volume as “CTAxs”, with `x´ standing for the assigned number and `s´ standing for “segmented”.

As a next step, a segmentation was created by selecting "Segment Editor" and adding a new segmentation X. The first segmentation was named "true lumen X" by double-clicking on “name” and with a double click on the color field, colored in "mass green". The second was named “false lumen X” and colored in “artery red”. In case of a significant thrombotic part, a third segmentation named “thrombus X” and colored in “thrombus red” was added. Figure 17 illustrates the previously described simpler approach to organize and store segmentations of the lumina by running all lumina under a single segmentation name. However, the alternative method involves saving separate segmentations for each lumen. The two options are equally useful, but show two main differences. Lumina in the second variant can be saved individually instead of only one dataset. Additionally, in the first variant, it is impossible to mark the same field in the CTA as both true and false lumen, as the previously marked parts are automatically overwritten. In comparison, overlapping of the lumina in the second variant was possible and, therefore, had to be avoided. Within the 40 segmented CTAs, significant variations appeared between the variants, depending on which team member performed the segmentation and whether they were processed at the beginning or the end of the project.

From this point onward, the actual segmentation started by opening the module “segment editor”, offering a great variety of segmentation tools, as shown in figure 16.

Within the 40 segmented CTAs, variations appear between the segmentation methods, depending on which team member performed segmentation. These included the functions "Local Threshold", "Plant Seeds", and "Fill between Slices". However, the final results did

not differ from each other, and it was impossible to determine which method was used for segmentation.

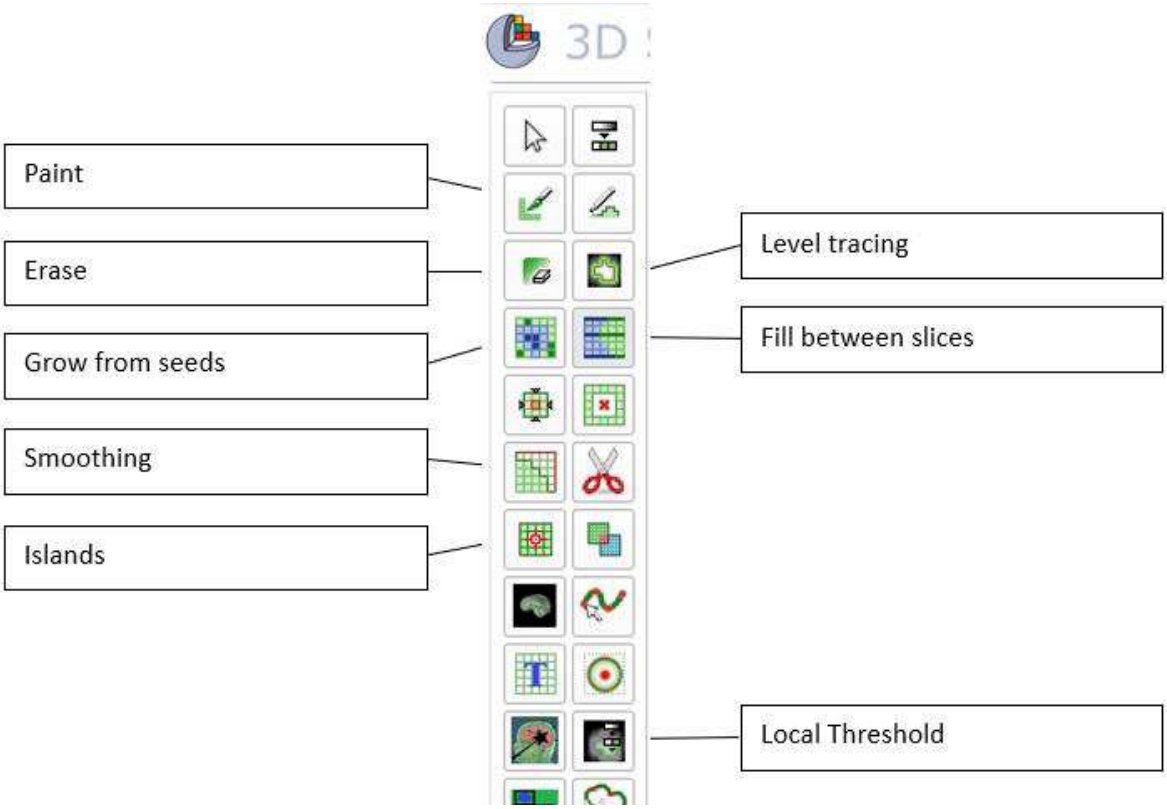

Figure 16: Different segmentation tools in the program “3D Slicer” within the module “Segment editor”, source: Screenshot from “3DSlicer” by author

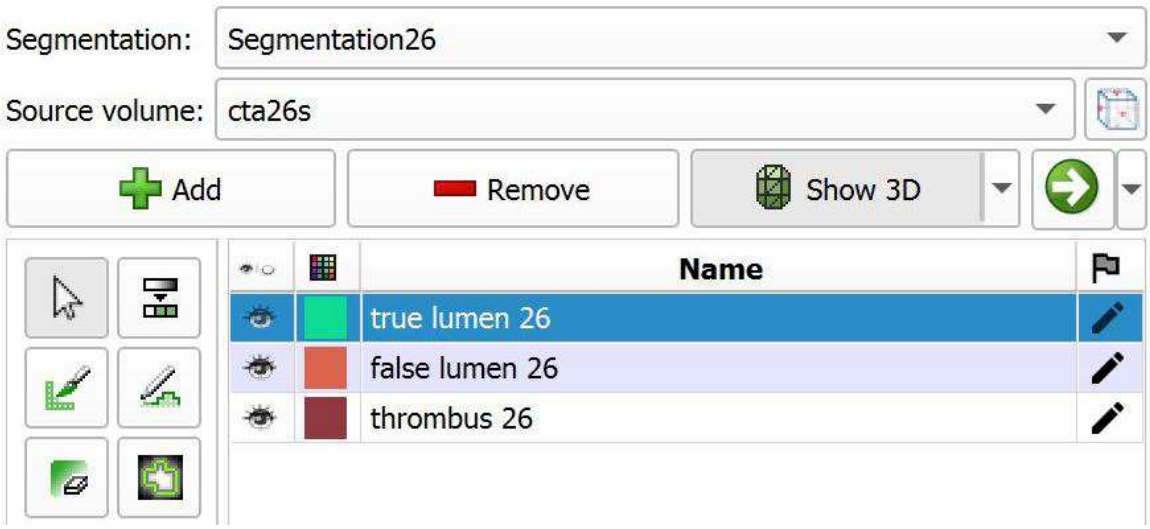

Figure 17: View of the segmentation name and added sub- segmentations with true, false and thrombus lumen, source: screenshot from “3DSlicer” by author

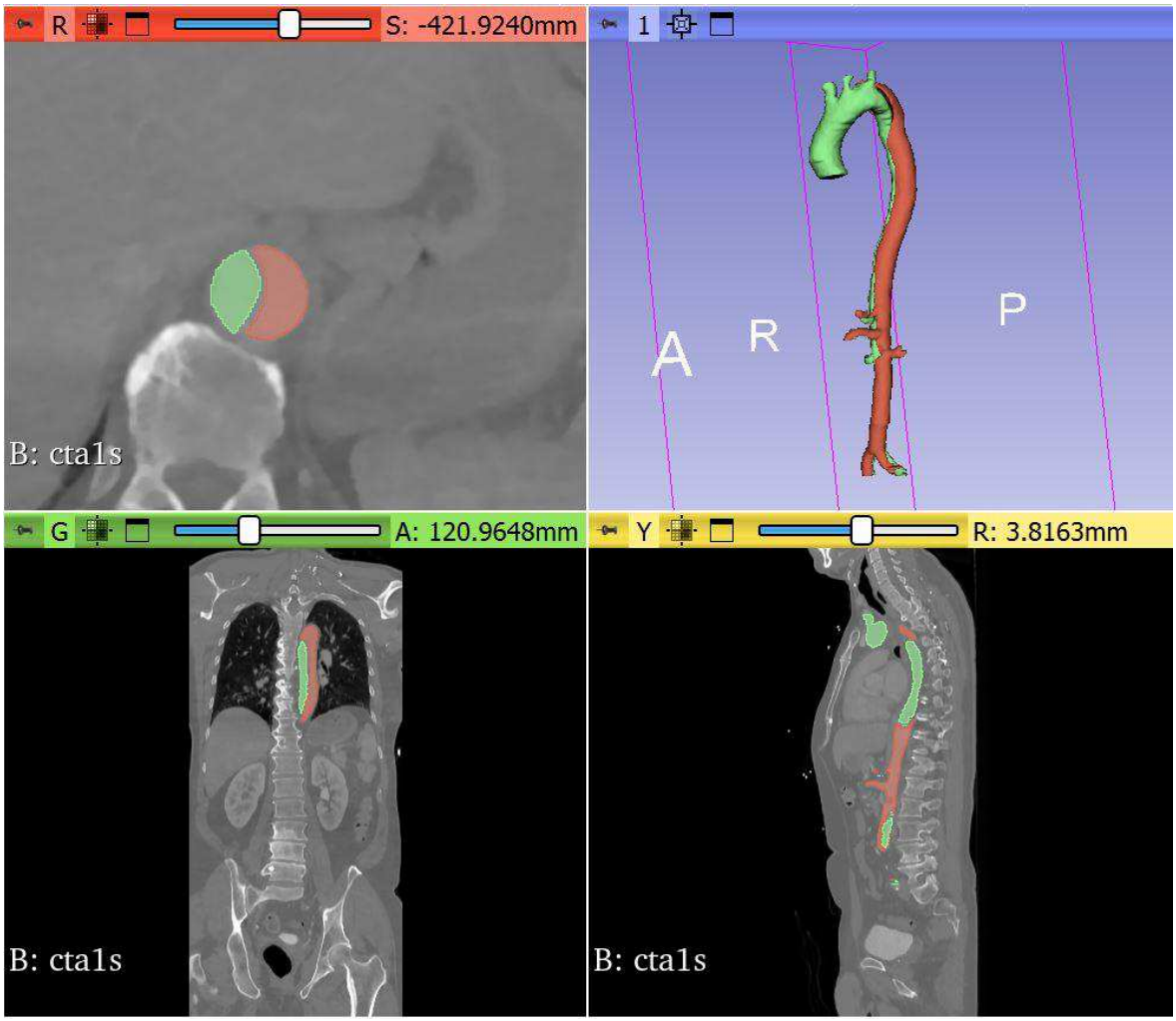

Figure 18: 4 window view of CTA 1 in the program “3D Slicer, showing the CTA scan in horizontal (red), frontal (green), sagittal (yellow) plane and the final segmentation (blue), source: screenshot from “3DSlicer” by author

Method 1: Local Thresholding

Since the method using the tools “Local Threshold” and “Islands” was demonstrated in tutorial videos of our technician, it was used for the majority of segmentations. Therefore, its detailed explanation encompasses all methods to the greatest extent. However, due to threshold differences, noise, and artifacts, this method requires substantial manual post-processing using the tools “paint” and “erase”. This strategy was successfully introduced for aortic aneurysms [53]; however, as ADs are more complex and artifact-rich anatomical structures, this method is limited in terms of usability. Nevertheless, the method performed well in several cases and was overall faster than complete manual segmentation [52]. After opening the segment editor, the subsequent course of action is as follows:

1. The segmentation algorithm field was set to “Grow Cut” and the minimum diameter was set to 3.0 mm. To create a first visual the tool, "Local Threshold" was

selected. Then, a favorable perspective with good vision of the aorta in one of the three planes in the CTA scan, such as the aortic bow in the horizontal plane, was configured. The desired part of the aorta, preferably focused on the targeted lumen of the dissection, was subsequently marked using “Ctrl” and a right mouse click. The visual preview should be enabled by clicking “Show in 3D”. By specifying a local threshold range manually through masking, the tool was selected until the entire aorta or one lumen was fully represented. Even though the order does not matter in the final segmentation, it is recommended to start with the true lumen, since the aortic areas outside of the type B dissection, such as the ascending aorta, are considered part of the true lumen.

2. In the next step, unwanted parts were erased. “Unwanted” was defined as every other structure or tissue outside the aorta, as well as all parts distal to the bifurcation and main parts of the aortic branches, following the ground rules described earlier. Additionally, the nontargeted lumen had to be erased in the segmentation. To erase, “Erase” was selected in tools, enabling the mouse to become a rubber, deleting all markings in the CTA that were clicked on. Minor misannotations or incorrect segmentation, which extend only through a few layers, were easily erased by choosing the affected layers and editing them manually.
3. For larger unwanted markings, extending through many layers, such as the complete course of renal arteries or the heart, the “Islands” tool saved time and work. This was achieved by identifying the layer that connects the intended part with the unintended marking. In this specific layer, the "erase" tool was utilized to remove all untargeted annotations, creating a gap in the overall image. It was important to ensure that a gap existed in all three planes and that the parts were completely separated from each other. Subsequently, the “Islands” tool was selected. In this setting, “keep the largest island” was enabled and confirmed by clicking “apply”. As a result, all parts or so called “islands” outside of the main segmentation were deleted.
4. Once the rough outline of the targeted lumen is established, detailed manual correction was started. By using the tools “Paint” and “Erase”, the entire segmentation was scrolled through layer by layer in horizontal plane, correcting and editing the lumen.
5. After completing the segmentation of the first lumen, the second lumen was started. Therefore, the other sub-segmentation was selected, and Steps 1 to 4 were repeated.

Method 2: Interpolating

An alternative approach was to utilize the tool “Fill between slices”. The main idea of this tool is to interpolate segmentations between manual slices of the CTA scan. Using this method, initially an axial segmentation is performed manually by using the “paint” tool every three to fiffteen slices depending on the amount of local tortuosity and cross-sectional change. Every 15th layer is manually segmented in mostly straight parts with clear outlines and few artifacts, every 10th layer in curved parts or parts containing more artifacts and every 3-5th layer in quickly changing parts such as kinking aortas, dissection flaps, or cases containing a high artifact rate.

In some cases, the pre-selection before applying “fill between slices” can be simplified with “level tracing”. This function attempts to draw a closed path within the same intensity range back to the starting point and, therefore, recognizes the luminal borders automatically. However, the efficiency of this tool is higher in CTA scans with a low artifact rate, which is more likely in healthy aortas [53].

Subsequently, the tool “fill between slices” is chosen to interpolate the slices. In the settings of this tool, first “Initialize”, then “Show 3D” and finally “Apply” were selected to activate interpolation. Consequently, the function interpolates the shape of the target structure along the two to fourteen slices that were previously skipped. After checking the preview of the results, manual corrections of incorrectly segmented slices were made, and the function was executed as a consequence.

This approach performed particularly well in long and straight parts of the aorta. Nevertheless, manual refinement using “paint” and “erase” was required in several areas. Especially in the aortic arch, parts with several branching vessels, the origin and termination of dissection flaps, as well as areas with more aortic kinking, further editing was required. However, segmentation times using this method tended to be lower than segmentation times performed with local thresholding, as shown in Table 2.

Method 3: Planting seeds

The third approach is similar to interpolation between slices. Here, the “grow from seeds” tool was used. Using the “paint” function, manual seeds are drawn in each region that should belong to a separate segment such as the true lumen, false lumen, and eventually thrombus. The seeds were planted at distances similar to those of the painted segments used in the previous method.

By clicking “initialize” followed by “Show 3D”, the function is initialized, and a preview is shown. Areas that were not correctly segmented in the preview can be corrected by switching to “paint” again and planting more seeds in the misclassified region. Once the preview yields a satisfactory image, the function can be confirmed and executed by selecting "apply” [52].

11. Results

11.1 Comprehensive Results Analysis

Patient selection did not depend on demographic or other patient-specific data. Instead, important aspects were the quality of the CTA scan, diagnosis of Stanford type B aortic dissection, and complexity of the dissection. However, general information about the patients, such as sex and age, was collected.

Table 1 shows the segmentation number with markings for segmentations performed by the author, age in years, sex, CTA slice thickness in millimeters (mm), diameter of the ascending aorta (mm), diameter of the descending aorta (mm), and complexity of segmentation. Furthermore, either “yes” or “no” was answered to the questions if the dissection was complicated, if there was aortic kinking, if the false lumen was larger than the true lumen, if the shape of the dissection was helical, if there was an interluminal gap, if there was more than 1 or 1 abdominal aortic branch affected by dissection, and if the iliac arteries were affected. The complexity of the dissection itself was defined according to the ACC/AHA 2022 guidelines [34]. However, the complexity of the segmentation could not be answered with “yes” or “no”. Instead, three categories with “simple” for 13 segmentations, “intermediate” for 15 segmentations and “complex” for 12 segmentations were established. The categorization did not only depend on the complexity of the dissection, but was also classified by the segmentation time, and anatomic characteristics, such as the involvement of abdominal aortic branches, or the existence of an interluminal gap or aortic kinking.

Among the 40 patients, 70% were male, and the average age was 62.5 years with a standard deviation of 12.2 years. Table 1 provides the following information:

- 9 patients (22.5%) with visceral arteries originating from the false lumen
- 25 patients (62.5%) with one or more renal arteries included in dissection
- 26 patients (65.0%) with a dissection extending into the iliac arteries
- 9 patients (22.5%) with pronounced aortic kinking
- 9 patients (22,5%) with helical lumen configuration

All selected patients were diagnosed with type B aortic dissection, with 15 individuals (37.5%) classified as having a complex aortic disease according to the ACC/AHA 2022 guidelines. Four (10%) complicated cases showed an increased risk of rupture, and in two patients (5.0%) visceral or renal malperfusion, leg ischemia, neurologic deficits, and uncontrolled hypertension occurred [34, 55].

Out of the 15 complicated cases, only five were defined as a “complex” segmentation. This suggests that there is no clear correlation between the clinical presentation of severity and the degree of complexity of the segmentation process. In addition, it is worth noting that two CTAs were classified as “simple” (CTA2 and CTA30). Conversely, CTA4 and CTA8 were categorized as "complex" segmentations despite lacking clinical complications, as per the definition.

Table 2 displays the segmentation volumes of true and false lumen in cubic centimeters (cm3), the mean Hounsfield Units (HU) in combination with the standard deviation for the true and false lumen, the segmentation time (ST) in minutes, and the segmentation method (SM). The methods include “Local Thresholding” with 13 segmentations, “Interpolating” with 19 segmentations, and “Region growing” with 8 segmentations.

Table 2 lists the time required for each segmentation. In total, 6260 minutes, equivalent to 104.3 hours, were required for the segmentation of 40 CTA scans. However, it is important to note that this duration does not include the time used for data collection, data conversion, or the learning process associated with the utilization of segmentation programs. On average, 156.5 minutes were spent per segmentation. The longest duration was for patient number 26 (330 min), followed by patient number 37 (300 min). The shortest recorded time was for patient 22 (40 min), followed by patient 20 (50 min).

Patient	Age [years]	Sex	Complicated dissection*	3D Dissection Morphology CT slice thickness [mm]	$\varnothing_{AscAo}$ [mm]	$\varnothing_{DescAo}$ [mm]	Aortic kinking	Larger false than true lumen	Helical dissection shape	Interluminal gap	≥ 1 abdominal aortic branch	AD into iliac arteries	AD segmentation complexity
1▽	50	male	no	2.0	36	29	no	yes	no	no	yes	yes	simple
2▽	61	female	yes	2.0	34	34	no	yes	no	no	yes	yes	simple
3▽	53	male	yes	2.0	37	45	no	yes	no	no	yes	yes	complex
4▽	71	male	no	2.5	45	37	no	yes	yes	no	yes	no	complex
5▽	65	male	no	2.0	43	33	no	yes	no	no	yes	yes	simple
6▽	53	male	yes	2.5	44	35	no	yes	yes	no	yes	yes	intermediate
7▽	77	male	yes	2.0	39	37	no	no	no	no	no	no	complex
8▽	73	male	no	2.0	39	34	no	no	no	no	no	no	complex
9▽	47	male	no	3.0	36	24	no	yes	no	yes	no	no	simple
10▽	58	male	no	3.0	42	34	no	yes	yes	no	no	no	intermediate
11	66	female	no	3.0	32	32	no	no	no	yes	yes	yes	simple
12	76	male	no	3.0	41	33	no	no	no	yes	yes	yes	intermediate
13	59	male	no	3.0	32	46	yes	yes	no	yes	yes	yes	complex
14	40	male	yes	2.0	32	32	no	yes	no	no	no	yes	intermediate
15	48	male	yes	2.0	35	33	no	yes	no	no	yes	yes	intermediate
16	71	female	no	4.0	33	34	no	yes	yes	yes	yes	yes	intermediate
17	66	male	yes	2.0	43	42	no	yes	yes	yes	no	yes	complex
18	58	male	yes	3.0	40	37	yes	yes	yes	no	yes	yes	complex
19	78	male	yes	2.0	39	38	yes	yes	no	yes	no	yes	intermediate
20	63	male	no	2.0	34	30	no	yes	no	no	no	no	simple
21	80	male	no	3.0	46	67	yes	no	no	yes	no	no	complex
22	76	female	no	3.0	37	34	no	yes	no	yes	yes	yes	simple
23	42	female	no	2.0	34	30	no	yes	yes	no	yes	no	intermediate
24	85	male	yes	3.0	37	36	no	no	no	no	no	yes	intermediate
25	55	male	no	30.	35	38	no	yes	no	yes	yes	no	intermediate
26▽	61	male	no	3.0	38	36	yes	yes	yes	yes	yes	no	complex
27▽	69	female	no	3.0	37	34	no	yes	no	yes	no	no	complex
28▽	68	female	yes	2.0	37	36	yes	yes	yes	no	yes	yes	intermediate
29▽	60	male	yes	3.0	35	35	no	yes	no	no	yes	yes	intermediate
30	47	male	yes	3.0	41	30	no	yes	no	yes	yes	yes	simple
31	66	female	no	2.0	42	37	no	yes	no	yes	Yes	yes	simple
32	62	male	no	2.0	38	35	no	yes	no	no	yes	yes	complex
33	36	female	no	2.0	31	30	no	yes	no	yes	yes	yes	simple
34	44	male	yes	2.5	36	35	no	yes	no	no	yes	no	complex
35	58	male	yes	3.0	40	34	no	yes	no	no	yes	yes	intermediate
36	63	male	no	3.0	30	32	no	yes	no	no	yes	no	intermediate
37▽	75	male	no	3.0	47	40	yes	yes	no	yes	yes	yes	intermediate
38	62	female	no	3.0	32	34	no	yes	no	no	yes	yes	simple
39▽	78	female	no	3.0	36	29	no	yes	no	no	yes	no	simple
40	79	female	no	2.0	33	25	no	yes	no	yes	yes	yes	simple

*Table 1: Abbreviations: 3D: three-dimensional, SD: ⌀AscAo, diameter of ascending aorta; ⌀DescAo: diameter of descending aorta; AD: aortic dissection, * defined according to ACC/AHA 2022 guideline, ▽ segmented by author, source:[34, 52]*

Patient	Segmentation volume TL [cm3]	Segmentation volume FL [cm3]	Mean HU ± SD TL	Mean HU ± SD FL	Segmentation time [min]	Segmentation method
1▽	184,8	122,8	230 ± 34	322 ± 67	180	Local Thresholding
2▽	186,1	204,1	280 ± 85	274 ± 67	180	Local Thresholding
3▽	217,5	381,34	324 ± 58	221 ± 52	280	Local Thresholding
4▽	309,3	178,4	208 ± 37	94 ± 59	225	Interpolating
5▽	178,4	181,6	257 ± 45	256 ± 42	165	Interpolating
6▽	204,0	212,2	233 ± 60	231 ± 48	210	Local Thresholding
7▽	271,0	122,1	273 ± 57	185 ± 50	150	Local Thresholding
8▽	387,8	81,6	233 ± 60	57 ± 64	180	Interpolating
9▽	172,8	136,5	266 ± 40	246 ± 33	210	Local Thresholding
10▽	254,9	75,6	255 ± 44	178 ± 61	240	Local Thresholding
11	184,3	88,2	212 ± 35	202 ± 41	150	Region growing
12	315,0	124,7	366 ± 91	312 ± 60	145	Region growing
13	290,5	393,1	243 ± 42	239 ± 33	215	Region growing
14	136,5	130,4	331 ± 45	277 ± 70	135	Region growing
15	182,8	150,9	244 ± 34	164 ± 84	115	Region growing
16	181,8	110,4	352 ± 54	131 ± 89	55	Interpolating
17	254,1	358,2	281 ± 24	118 ± 80	80	Interpolating
18	331,5	279,2	229 ± 46	195 ± 44	70	Interpolating
19	375,8	170,3	279 ± 56	104 ± 54	70	Interpolating
20	194,8	121,2	386 ± 83	192 ± 128	50	Interpolating
21	385,3	437,8	241 ± 104	271 ± 38	85	Interpolating
22	287,7	166,8	229 ± 46	221 ± 58	40	Interpolating
23	204,9	138,0	402 ± 32	246 ± 86	290	Local thresholding
24	311,7	124,8	422 ± 133	256 ± 112	95	Interpolating
25	196,7	94,8	248 ± 21	201 ± 22	280	Local Thresholding
26▽	434,6	244,4	224 ± 52	259 ± 47	330	Local Thresholding
27▽	253,9	70,1	431 ± 60	386 ± 62	180	Local Thresholding
28▽	258,9	198,9	233 ± 46	105 ± 54	255	Local Thresholding
29▽	199,3	216,5	402 ± 66	308 ± 68	150	Local Thresholding
30	209,7	135,6	305 ± 47	293 ± 31	120	Interpolating
31	202,1	228,8	357 ± 59	284 ± 49	140	Interpolating
32	282,3	161,1	110 ± 31	149 ± 27	110	Interpolating
33	154,1	110,8	342 ± 47	255 ± 67	100	Interpolating
34	183,0	171,4	229 ± 44	188 ± 25	95	Interpolating
35	242,9	144,7	262 ± 51	114 ± 59	105	Region growing
36	212,1	111,0	160 ± 51	203 ± 50	130	Region growing
37▽	357,3	304,3	298 ± 57	234 ± 42	300	Interpolating
38	196,3	112,2	285 ± 68	252 ± 49	95	Region growing
39▽	231,0	115,6	500 ± 85	439 ± 81	150	Interpolating
40	218,5	53,7	424 ± 68	352 ± 45	105	Interpolating

Table 2: Segmentation volumes, voxels, and Hounsfield Units (HU) with standard deviation (SD) plus segmentation times and method. Abbreviations: TL, true lumen; FL, false lumen; HU, Hounsfield Units; SD, standard deviation, ▽segmented by the author, source: [52]

12. Discussion

12.1 Problems occurring with “SimVascular”

Apparently, certain difficulties during the segmentation process using “SimVascular” arose, all ultimately resulting in inaccuracies in the results and a significant lengthening of the overall process.

The inaccuracy of the completed segmentation results from various causes. Initially, every fifth layer of the CTA scan was segmented by outlining the lumina. However, several outlined layers had to be deleted due to overlapping with previous or succeeding outlines. In particular, the aortic arch and general curvatures in the aorta show major overlapping issues. As a result, layers had to be reduced drastically in these areas for the program to create a 3D view segmentation. As shown in figure 15, only a fraction of the original layers remained, exhibiting infrequent distances from one another. The segmented layers varied between every 10th and 40th layer. In areas such as the aortic arch or in cases where the aorta shows kinking, substantial gaps exist between outlines. Consequently, the program filled these gaps by supplementing them based on the marked path. These automatically segmented outlines show various inaccuracies that cannot be edited. Additionally, in four out of five segmentations it was impossible to create the beginning of the dissection due to this issue.

Another problem leading to inaccuracy was the difficulty of editing the outlines. Since it was only possible to edit the layers, which the user had created manually, many layers remained not editable. The only option to change or correct inaccurate automatically filled layers was to edit the nearest manual layer. The outcome of any small edit was unpredictable, since the segmentation was either optimized or worsened without a reason known.

In addition, segmenting aortic vascular branches proved to be challenging due to numerous overlaps at the branching points. To address this issue, individual paths with corresponding segmentation must be created. This process would have been excessively time-consuming. Branches such as the left subclavian artery or the bifurcation of the femoral arteries would have been crucial for recognizing an aortic dissection as a Stanford type B dissection and for gaining an understanding of the extent of the dissection.

After marking the lumina and creating a path through the dissection for segmentation, the program switched to the segmentation mode. In this mode, the program displays only the cross-section of the CTA and zooms in the region where the path is marked. Because segmentation is confined to this small area of CTA and requires fine detailed work, this

zoom feature is advantageous. However, the program exhibited instances in which it did not show the entire area surrounding the mark. Although the path marker was centered in the targeted lumen, a part of the aorta, including the lumen, was missing. This issue was due to an error in the software and did not occur on every computer. Consequently, the layers with missing parts in the CTA image could not be segmented manually, which subsequently led to distances between the outlined slices and major inaccuracies.

The creation of the path and the outlining of the layers seemed to be the core part of the process, taking only 1.5 hours. However, the subsequent editing, correction, and rectifying of errors appear to be time-consuming, with certain CTA scans requiring several additional hours. The reason for this extended duration was on one hand attributed to the already mentioned unpredictable outcomes of small edits, and on the other hand, to the loading time and complexity of the lofting preview. To edit the parameters, path, or outlines of the segmentation, the 3D lofting preview had to be disabled. Consequently, the preview had to be closed and reloaded after every editing. This reloading time would take up to four minutes. Even though this problem was most likely due to the slow processor of the laptop being used, it remained a significant factor that could not be easily altered and significantly complicated the process.

In summary, the lack of the targeted accuracy and the cumulative challenges mentioned, prompted the team to decide against further pursuing segmentations using the program “SimVascular”.

12.2 Comparison Table 1 and 2

Notable differences in segmentation time were observed among team members, particularly between the author and junior cardiac surgeons. As displayed in table 2, 16 CTA scans were marked with “▿“, indicating that the author performed the segmentation. Upon comparing segmentation times, it is evident that two of the three longest durations are associated with these markings. Furthermore, the average segmentation time for the authors segmentations is 211.56 minutes, which is 55 minutes longer than the overall average. Possible reasons include the lack of experience in diagnosing aortic dissections, lack of familiarity with CTA scans, and the resulting insecurity in decision-making as a medical student. Another plausible reason is the segmentation method, since the method “Local Thresholding” was primarily used by the author. As described in the “Material and Methods” section, this method was exemplified in tutorial videos of our technician and was therefore used for the

majority of segmentations during the learning process of the program. Owing to threshold differences, noise, and artifacts, this method requires a greater amount of manual editing than other semi-automatic methods. As evidence, CTA 23 was not segmented by the author, but performed through the "Local threshold" method, resulting in the third-longest segmentation time of 290 minutes.

Comparing Tables 1 and 2, no notable connection between the segmentation time and the complexity of the segmentation or dissection was discovered. Although there might be a correlation between “simple” segmentations without complications and a short segmentation time, an equal connection between “complex” segmentations of complicated ADs and a long segmentation time cannot be made. The three shortest segmentation times were in CTAs without any clinical complications, wherein two out of three were classified as “simple” (CTA 20 and CTA 22), and one as “intermediate” (CTA 16). In contrast, among the three CTAs with the longest segmentation times (CTA 23, 26, and 37), none was characterized as complicated according to the AHA guidelines 2021 [40]. Additionally, only one of them was categorized as a "complex" segmentation, while the remaining two were categorized as "intermediate". Consequently, a definitive correlation cannot be established without further statistical testing, and alternative factors, such as the segmentation method, are more likely contributors to prolonged segmentation times.

12.3 Individual description of the segmentations

The completed CTA segmentations 1-10, 26-29, 37, and 39 are presented in images 19 – 36, accompanied by detailed descriptions of the individual segmentation processes. This encompasses a comprehensive overview, incorporating descriptions of challenges encountered during segmentation, the employed segmentation method, duration and anatomic aspects of the aorta, and dissection. While the images of the segmentations [figure 19-36] are limited to a 2D view, it is important to note that the actual segmentations are 3D presentations with the possibility of rotating the model and the capability of selectively displaying or concealing individual lumens. Therefore, a brief 15-second observation provides a concise yet informative impression of the dissection.

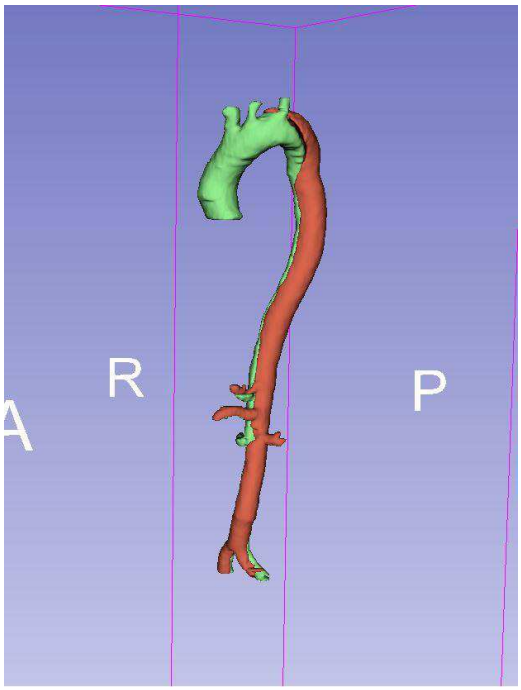

Figure 19: 3D segmentation of CTA 1, source: Screenshot from "3DSlicer" by author

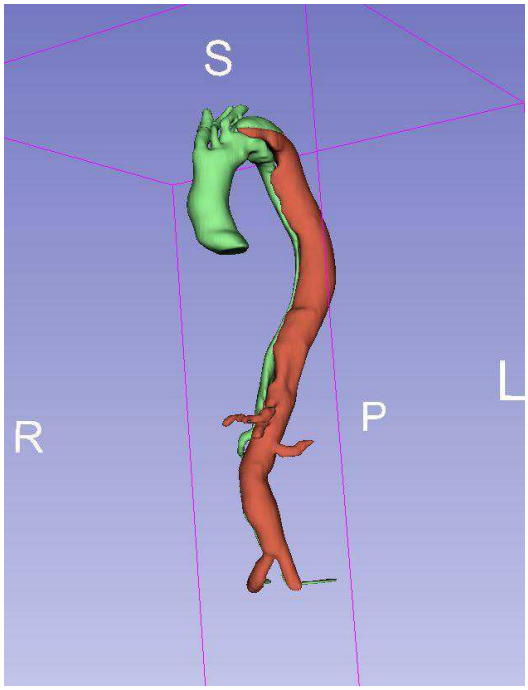

Figure 20: 3D segmentation of CTA 2, source: Screenshot from "3DSlicer" by author

- CTA 1: Although the dissection of patient number 1 was not defined as complicated and the segmentation process went swiftly, the total segmentation time of 180 minutes surpassed the average. A plausible explanation for this deviation is the fact that it was the initial CTA scan segmented using the program "3DSlicer". As a result, there was no established routine, and the program was newly acquired and learned. Furthermore, the segmentation method "Local Thresholding" was used, being the most time–consuming of the three methods. Figure 19 shows the completed 3D segmentation. In this case, there was no aortic abnormality; however, the dissection affected most of the abdominal aortic branches and both iliac arteries.
- CTA 2: Even though the aortic dissection in CTA 2 is defined as complicated, the segmentation process was listed as "simple". However, due to the segmentation method using "Local Threshold" the segmentation time was 180 minutes. As displayed in figure 20, the abdominal aortic branches and both iliac arteries are affected by the dissection, partly originating from the false lumen.

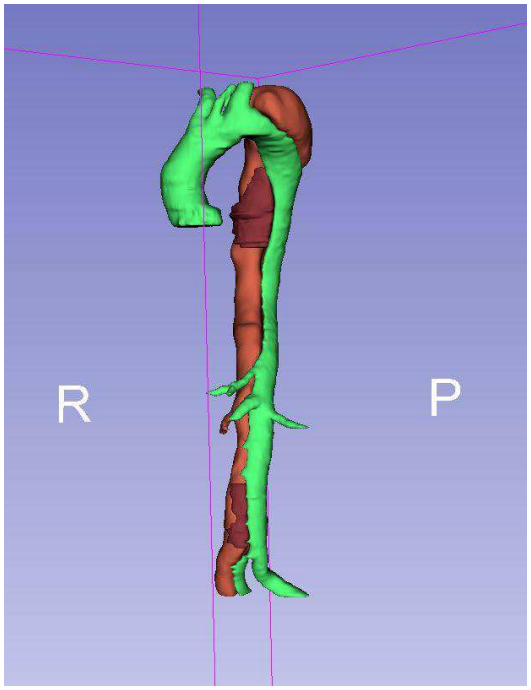

Figure 21: 3D segmentation of CTA 3, source: Screenshot from "3DSlicer" by author

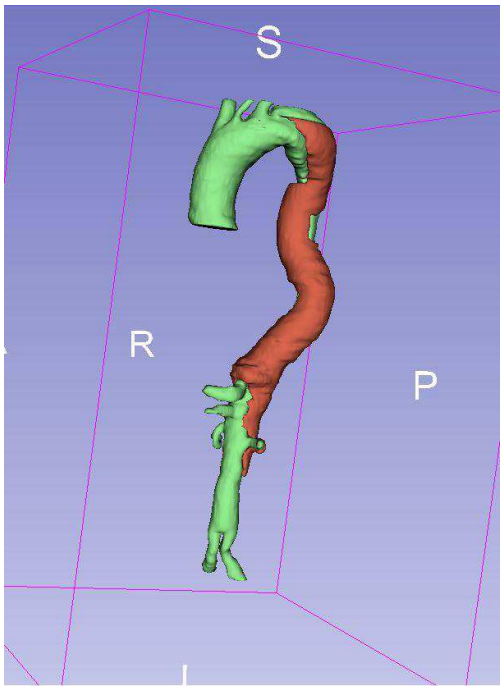

Figure 22: 3D segmentation of CTA 4, source: Screenshot from "3DSlicer" by author

- CTA 3: In this segmentation, a gap between the lumina existed, which was originally marked as a new segmentation in a dark-red color and was considered a thrombus. As further explained later, these allegedly named thrombi were subsequently removed owing to inadequate definitions, blurred slices, and inconsistencies in the segmentations. In this case, the segmentation time of 280 minutes aligns with the complexity of the segmentation, substantiating the designation of this dissection as complicated. As presented in figure 21, some abdominal branches and one iliac artery are included.
- CTA 4: Even though CTA 4 [figure 22] was not defined as a complex AD, the segmentation process appeared to be complicated and was therefore listed as "complex". Appropriately, 225 minutes were required. Furthermore, the differentiation between true and false lumen proved to be challenging in the majority of the CTA scans. This aortic dissection terminates in the abdominal part of the aorta, and as a result, does not impact the iliac arteries. Nevertheless, the branches of the aortic abdominal region were only partially affected. This was the initial CTA using the method "Interpolating".

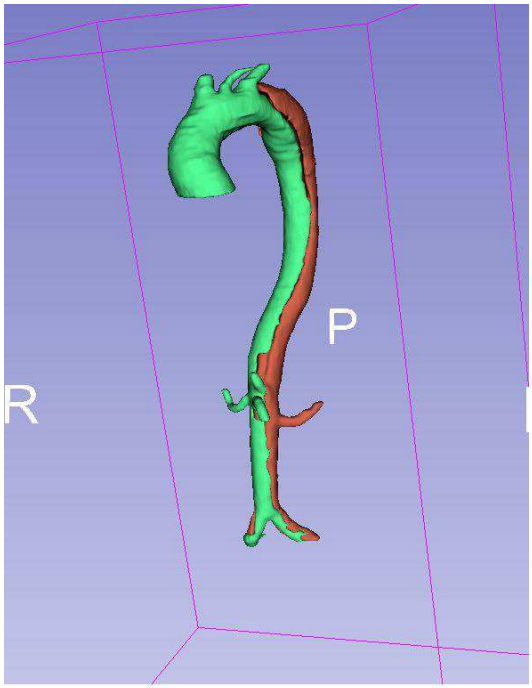

Figure 24: 3D segmentation of CTA 5, source: Screenshot from "3DSlicer" by author

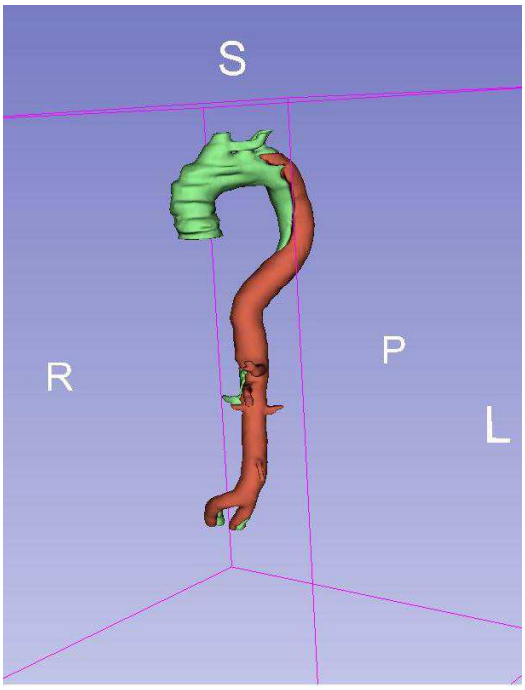

Figure 23: 3D segmentation of CTA 6, source: Screenshot from "3DSlicer" by author

- CTA 5: As displayed in figure 24, CTA 5 was a simple segmentation with no complexity. Although the 165 minutes required for segmentation slightly exceeded the mean, this represents one of the briefer segmentation times achieved by the author. In this case, the dissection extends through the entire descending aorta, affecting some of the abdominal aortic branches and both iliac arteries. Similar to CTA 4, the method "Interpolating" was used.
- CTA 6: CTA 6 was defined as a complex aortic dissection and the segmentation complexity appeared to be "intermediate". However, the difficulties encountered during the segmentation process and the comparatively long segmentation time of 210 minutes were not due to a complex aortic dissection. Instead, they were primarily associated with the distinctive anatomy of the branches of the aortic arch and artifacts present in the ascending aorta. As shown in figure 23, the ascending aorta consequently appears edged, and only two branches originate from the aortic arch. This anatomic variation occurs at a frequency of 9 percent, where the truncus brachiocephalicus and arteria carotis communis sinistra share the same stem [49]. Major parts of the abdominal aortic branches are affected, and the false lumen extends into both iliac arteries.

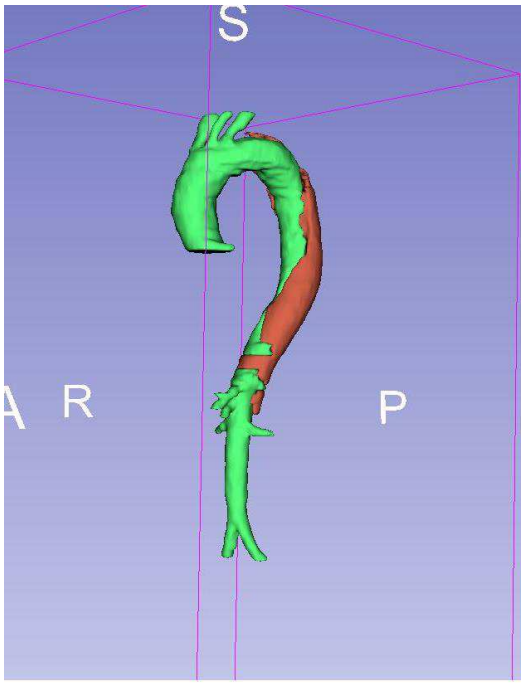

Figure 26: 3D segmentation of CTA 7, source: Screenshot from “3DSlicer” by author

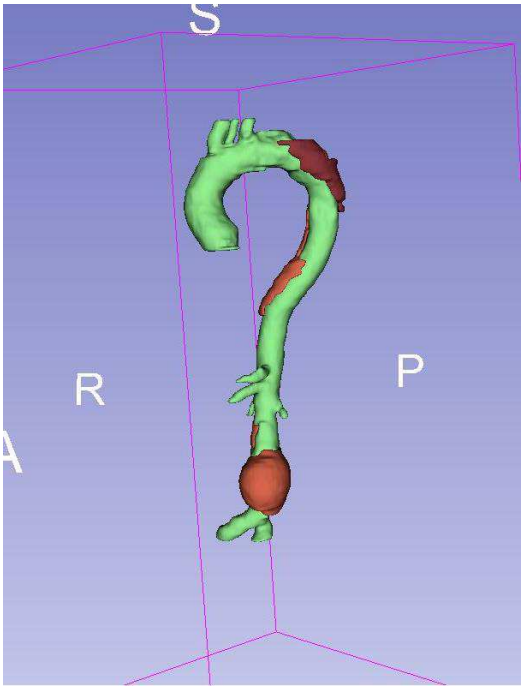

Figure 25: 3D segmentation of CTA 8, source: Screenshot from “3DSlicer” by author

- CTA 7: According to ACC/AHA 2022 guideline [34], CTA7 is defined as a complicated type B aortic dissection. Despite the segmentation time being 150 minutes, which is below the average, and the dissection not exhibiting distinctiveness in figure 26, the segmentation process was categorized as "complex", owing to the intricate nature of the dissection itself. Similar to CTA 4, the dissection does not extend throughout the entire descending aorta, and neither the abdominal aortic branches nor iliac arteries are affected.
- CTA 8: The dissection of patient 8 was not defined as complicated. However, the segmentation process appeared to be rather difficult and was therefore classified as “complex”. The challenges encountered arose from uncertain differentiation within the false lumen, making it difficult to discern whether the false lumen was patent or thrombosed. Although certain regions showed characteristics suggestive of thrombus, the transitions were indistinct. Even after the removal of all thrombus segmentations, manual determination of each CTA slice remained time-consuming. Even though CTA 8 was segmented with the method “Interpolating”, almost the whole segmentation of the false lumen was segmented manually slice-by-slice. The false lumen in the region between the renal and iliac arteries, which are all unaffected by dissection, is prominent in figure 25. Here, the diameter of the false lumen widened to the extent characteristic of an aneurysm within the false lumen.

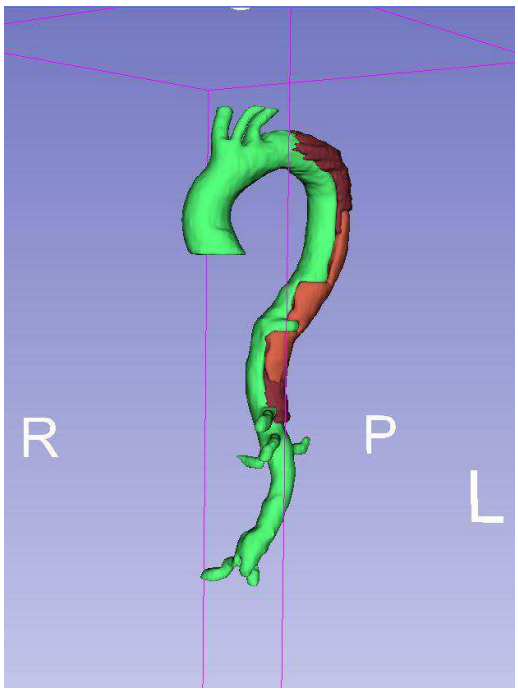

Figure 28: 3D segmentation of CTA 9, source: Screenshot from "3DSlicer" by author

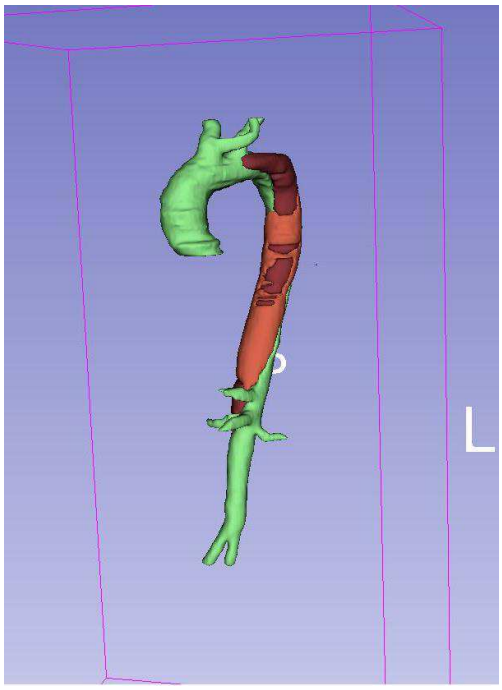

Figure 27: 3D segmentation of CTA 10, source: Screenshot from "3DSlicer"by author

- CTA 9: This CTA scan was neither defined as a complicated dissection, nor did the segmentation process appear to be complex. Therefore, this segmentation was listed as "simple". Nevertheless, the time used for segmentation exceeded the average by 53,5 minutes, primarily attributable to a prolonged project finalization and refinement process. Since it was decided to remove all thrombus segmentations, further editing and manual differentiation between false lumen and thrombus was required. As pictured in figure 28, the dissection depicted no involvement of the main aortic branches.
- CTA 10: Despite being categorized as "intermediate" and a non-complicated dissection, the segmentation process of CTA 10 [figure 27] was time-consuming, with a duration of 210 minutes. Similar to CTA 9 [figure 28], the reason was the segmentation of the presumed thrombus and the subsequent prolonged project finalization and refinement process. As evident in CTA 6 [figure 23], this patient also exhibits the anatomical variation of a combined truncus brachiocephalicus with the arteria carotis communis sinistra [49]. Specific difficulties appeared in the aortic arch, including defining the origin of the dissection and smoothing of the edges. In this aortic dissection, no aortic branches, including the iliac arteries, are affected.

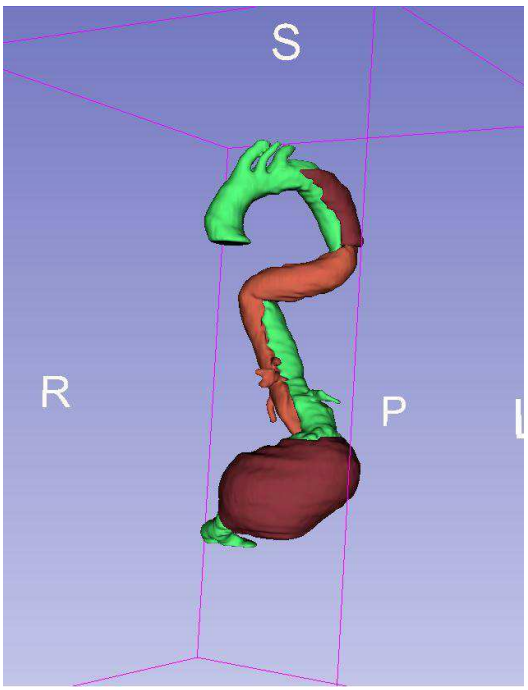

Figure 30: 3D segmentation of CTA 26 anterior view, source: Screenshots from "3DSlicer" by author

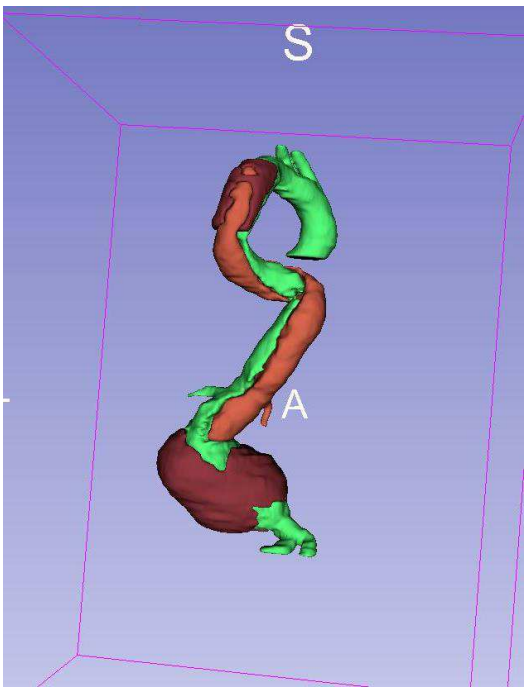

Figure 29: 3D segmentation of CTA 26 posterior view, source: Screenshots from "3DSlicer" by author

- CTA 26: In this instance, there was a negative correlation between the severity of dissection and the complexity of the segmentation. While it was not defined as complicated, the process of segmentation and editing the CTA proved to be complex, resulting in a segmentation time of 330 minutes, which is notably the longest. Owing to severe kinking of the aorta, it was necessary to add two screenshots [figures 29 and 30] of CTA 26 to this thesis, creating an improved spatial perception. Similar to CTA8 the false lumen/thrombus in the region between the renal and iliac arteries is widened to an aneurysmatic extent. Furthermore, the thrombus appears circular, surrounding the true lumen. As shown in figures 29 and 30, parts of the abdominal aortic branches are affected by dissection or even originated from the false lumen. The iliac arteries, however, are not included.
- CTA 27: Equally to CTA 26, the complexity of the clinic does not align with the complexity of the segmentation process. While the segmentation, shown in figure 32, appears to be smooth, the differentiation of lumina posed challenges, requiring manual definition in various sections. Moreover, the dissection exhibited partially thrombosed segments and additional entries/re-entries, creating dissection flaps. Therefore, notable pseudo-lumina due to motion artifacts caused by an oscillating dissection membrane appeared in the CTA. Even though the dissection extents to the proximal part of the left iliac artery, no other aortic branches are involved in the dissection.

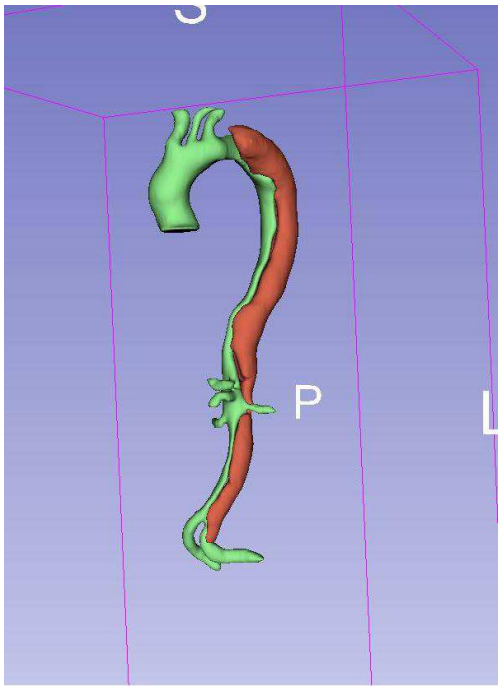

Figure 32: 3D segmentation of CTA 27, source: Screenshot from "3DSlicer" by author

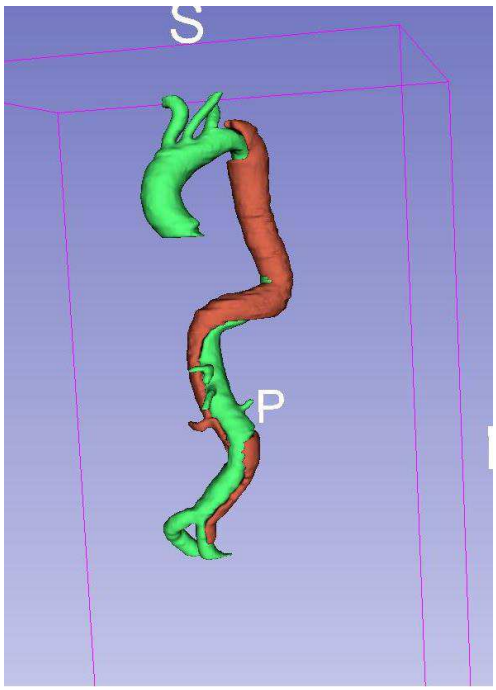

Figure 31: 3D segmentation of CTA 28, source: Screenshot from "3DSlicer" by author

- CTA 28: The aorta of patient number 28 shows severe kinking, resulting in a rather long segmentation time of 255 min. Even though the aortic dissection seen in figure 31 is defined as a complicated AD, the segmentation process was classified as "intermediate", since the automatic segmentation process recognized the lumina regardless of kinking. Additionally, some aortic branches, especially the right renal artery and the left iliac artery are affected by the dissection.

- CTA 29: CTA 29 was defined as a complicated aortic dissection and was therefore classified as an "intermediate" segmentation process. *Similar to CTA 6 and CTA 10, anatomical variations exist in the branches of the aortic arch.* As the aortic dissection does not extend through the entire descending aorta and terminates with the included truncus coeliacus, the dissection is comparatively short. Consequently, the segmentation time of 150 minutes is below average and one of the shortest segmentation times by the author [figure 34].

- CTA 39: In this case, no complicated dissection was present and the segmentation was classified as "simple", aligning with a segmentation time of 150 minutes. As displayed in figure 33, some abdominal aortic branches and the left iliac artery partly consist of a false lumen and are affected by dissection. Similar to CTA 27, a pseudo-lumen due to motion artifacts is evident, particularly in the region immediately following the LSA.

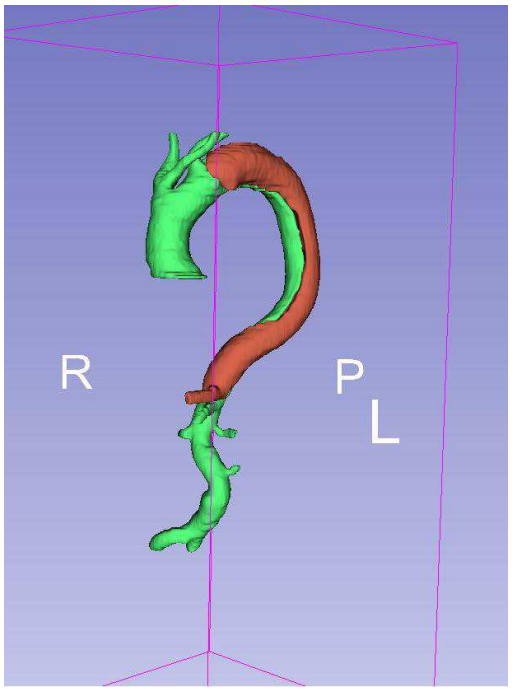

Figure 34: 3D segmentation of CTA 29, source: Screenshot from "3DSlicer" by author

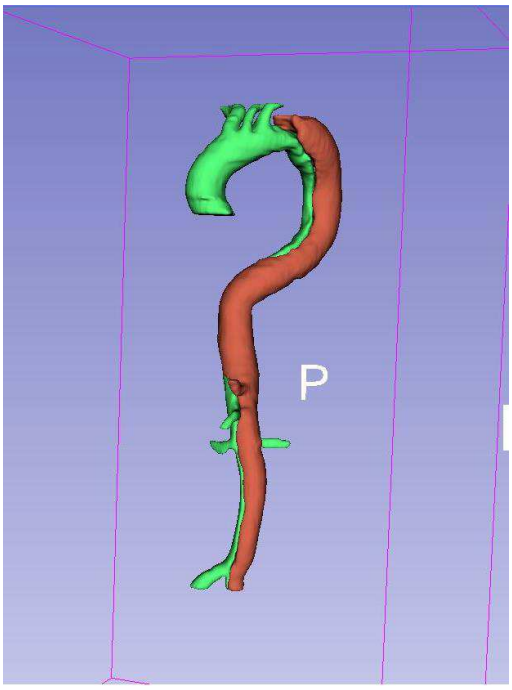

Figure 33: 3D segmentation of CTA 39, source: Screenshot from "3DSlicer" by author

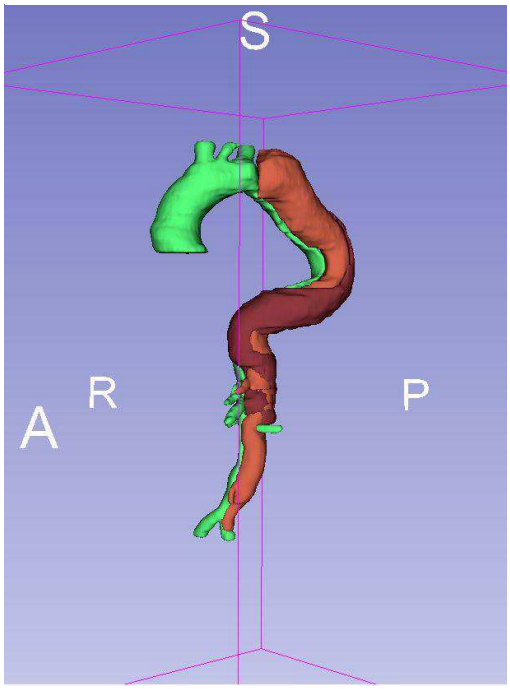

Figure 36: 3D segmentation of CTA 37 anterior view, source: screenshot from "3DSlicer" by author

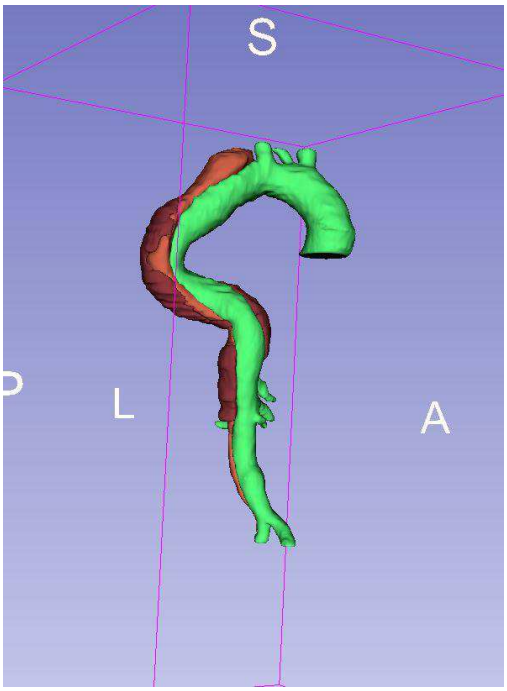

Figure 35: 3D segmentation of CTA 37 posterior view, source: screenshot from "3DSlicer" by author

- CTA 37: By adding two figures [33, 34], an improved spatial perception is created. This segmentation required the second-longest time, with a duration of 300 minutes. Furthermore, this AD shows aortic kinking and a partially thrombosed false lumen. However, the segmentation process was "intermediate", since the segmentation of the thrombus was removed. The aortic abdominal branches and left iliac artery are affected by the dissection.

12.4 Project Finalization and Refinement Process

In all different segmentation methods, manual post-processing using the tools “paint” and “erase” to optimize and correct the segmentations were required. The time needed to attain the desired result depended on multiple factors, such as the complexity of the dissection, the quality of the CTA scan, and consequently, the quality of semi-automatic segmenting. However, a majority of time was devoted to manual post-processing in all segmentations.

After completing the final editing, the segmented data could subsequently be saved by selecting "File" and choosing "Save Data." Then the desired storage location could be selected and storing could be activated by clicking "Save."

The segmentation time for yielding satisfactory results in healthy aortas varies between thirty and ninety minutes for “healthy” aortas, but can range up to six hours for pathologically CTA scans, shown in table 2. While the skill of the segmenting team member and the method used for segmentation might play a role in the overall time used for one CTA scan, high-quality CTA and a low rate of artifacts and pathological findings simplified and shortened the segmentation process [53].

12.5 Further improvement after review process

After the segmentation process, a senior cardiac surgeon checked the results. Additionally, an anonymous reviewer verified the segmented cases after handing in the paper “Type B Aortic Dissection CTA Collection with True and False Lumen Expert Annotations for the Development of AI-based Algorithms” by Dr. Christian Mayer, Antonio Pepe and the author et.al. [52].

CTA 1-10, 26-29, 37, and 39 were personally segmented by the author of this thesis and form the groundwork on which the detailed explanations in the discussion section are based. The remaining 24 of the 40 CTAs were segmented by other team members.

Based on both the feedback received and suggestions for corrections, as well as the comparison of the 40 segmentations among themselves, the segmentations were meticulously revised, layer by layer, and the following changes were implemented:

1. Segmentations of the aortic wall and calcifications were completely removed from the lumina, as they are not part of it.
2. Thrombus segmentations were removed in all the cases. This decision is primarily rooted in the challenge of definitively establishing whether a thrombus is present or

not, since the transitions between the true and false lumen were unclear and blurred in many cases. Furthermore, this approach ensures uniformity across all the segmentations. The thrombus segmentations were deleted in CTA 3, CTA 8, CTA 9, CTA 10, CTA 26, and CTA 37.

3. In CTA 1, attention was given to the true lumen. In the range of -460.92 to -481.92, a pseudo-lumen due to motion artifacts was mistakenly segmented as part of the false lumen. This error has been rectified. The celiac trunk and other branches were revisited and corrected.
4. CTA 2 showed unintended components in areas -975-989, -873, and particularly -689 – 697, which were corrected. In the distal region of the aortic arch, portions of the true lumen, that did not belong, were deleted from the segmentation. These parts were mostly left blank, as they could not be definitively attributed to either of the lumina. CTA 2 was modified twice based on the follow-up feedback. The lumen erroneously marked as true lumen in the range of -673 to -685 is now segmented as false lumen.
5. Missing segments of the false lumen in the small curvature in CTA 3 were added. Particularly in the regions -297.5 to -263.0 and -239.0 to -224.0, the false lumen was reduced, as there may have been partial thrombosis or wall involvement in these areas. At 480.5, all unintended structures were removed from the segmentations.
6. In the range of -346.2 to -358.2 in CTA 4, the portions that were erroneously marked as the true lumen were changed to the false lumen. Additionally, between -370.2 and -376.2, the pseudo-lumen was removed from the true lumen. The branches of the true lumen, especially at the celiac trunk ostium, were enhanced.
7. In CTA 5, missing pixels in the true lumen were added. In particular, the false lumen was refined and improved in the regions of -1123 to -1169.45 and -1307 to -1327.
8. CTA 6 showed parts that were erroneously marked as the true lumen and were consequently changed to the false lumen in the following areas:
    - -147 to -155.46
    - -299 to -287.96
    - -356.46 to -380

9. Given that CTA 26 exhibits a pronounced aneurysmal expansion in the area of -532 to -621, which was segmented as “thrombus” before, the segmentation appeared less accurate after the deletion of the thrombus segmentation. Since this area could not definitively be labelled as false lumen based on contrast differences, this region was then preserved as "thrombus” as part of the false lumen segmentation.

12.6 Future Research Directions and Possible Benefits of Aortic Segmentations

Although semi-automatic tools used for segmentations have improved the segmentation process and all 40 cases were successfully segmented, manual corrections were time-consuming. Since only well-trained medical staff are able to perform segmentations, and personal resources and time are limited in the clinical routine, fully automated segmentations could abbreviate the process of manually segmenting anatomic structures of interest. Subsequently, an automated process can reduce the required resources.

Following this thesis, a database containing segmented type B aortic dissections will be created. Subsequently, the goal is to expand the “ground-troth” database and distribute the annotated CTA dataset publicly for the development of effective deep learning-based algorithms and patient-specific simulation tools [56]. This automated deep-learning algorithm can be used to train and create automated segmentation algorithms. However, it is necessary to develop and validate algorithms applicable to healthy aortas first. In the future, the results could be extended to pathological aortas, as seen in aortic dissection. An interdisciplinary approach involving specialized physicians, engineers, biomedical materials, and computer scientists is needed to accomplish these goals [53].

The first possible benefit of automatic segmentations is that they could play a useful role in enhancing the understanding of complex morphologies and various aortic diseases. In cases of type B aortic dissections, where morphology can be complex, segmentations can aid in establishing the length of the tear, additional entries, re-entries, and flap extension. Furthermore, it could contribute to the differentiation of uncomplicated and complicated cases for appropriate therapeutic decisions. Through segmentation, evaluating different diameters of, for example, the ascending aorta, aortic arch, and descending aorta, is possible. Maximal aortic diameters, false lumen diameters, progressive enlargement of lumens, and the presence of calcifications or kinkings can be assessed more easily and rapidly. The detection of anatomical variations, such as an artery lusoria, proves valuable for

comprehensive assessments and offers useful insights for non-aortic interventions in seemingly healthy aortas [52].

Second, segmentations could play a vital role in interventional planning, particularly in the creation of custom-made stents and the sizing of implants for endovascular procedures. The segmentations can be converted into 3D-printed models and serve educational, interventional planning, and simulation purposes. Time-consuming preprocedural evaluations, including the necessity to size stent grafts, can be simplified through CTA segmentations and simulations. For optimal wall tension, preventing endoleaks and stent migration, especially in the development of patient-specific TEVAR devices, including biological or 3D-printed stents, achieving an accurate oversize is crucial. Furthermore, the evaluation of factors such as coverage of the left subclavian artery and vertebral artery anatomy play an important role. Preprocedural assessments of stent forces, biomechanical factors, and risk considerations, along with virtual stent-graft deployments, contribute to predicting altered loading conditions and optimizing outcomes [52].

Third, CTA evaluations could bring essential improvements not only in pre-interventional planning but also in post-TEVAR assessments, especially given the ongoing follow-ups required for aortic diseases. The current overflow in outpatient clinics for aortic diseases requires a more efficient approach. Ideally, fully automated segmentation of the complete aorta could not only simplify the identification of preprocedural pathologies, but also aid in long-term control of aortic dissections. This aspect includes the detection of disease progression, endoleaks, and TEVAR-related complications. In addition, predicting and monitoring thrombus formation in uncomplicated type B aortic dissections, as well as assessing ongoing perfusion after TEVAR procedures, are important yet time-consuming. Simulation and modeling techniques would offer insights into disease relationships and thrombus growth, while machine-learning-based algorithms provide lifelong monitoring of aortic morphology and pathologies in various patient conditions.

13. Limitations

Despite its strengths, this project has some limitations. Because the study population of 40 patients was rather small, it might not be representative of all patients with aortic dissection. Furthermore, the case selection process was mainly focused on CTA scans and quality, not on the patient. While this is an advantage for protecting the patient's anonymity, it also results in inconsistencies in the study population, such as an uneven gender distribution. A

larger sample size would provide a more representative study and more comprehensive picture of cases of aortic dissection.

Furthermore, although automated segmentation has potential clinical benefits, considerable progress is still required. Further segmentations are needed, and several algorithms need to be developed before segmentations can be used in routine clinical practice. Subsequently, their seamless integration into clinical workflows or widespread adoption in various healthcare settings may face practical challenges such as financial costs for implementation or the required training time of all team members.

Another limitation is the dependency of segmentation on user proficiency and experience. Since proficiency can influence the precision of manual interventions or adjustments in the segmentation process, human biases are possible. On one hand, the division of labor results in a reduction of human bias. On the other hand, however, differences in accuracy may exist in between the 40 cases, due to proficiency and experience of the segmenting person. Differences in accuracy were reduced by setting ground rules for the segmentation process and the main errors were corrected through feedback provided by anonymous reviewers. In future projects involving manual or semi-automatic segmentations, bias could be minimized by involving multiple individuals in the segmentation of one case.

14. Conclusion

The second part aimed to investigate the use of 3D imaging techniques in the diagnosis and management of type B aortic dissections. Specifically, this thesis focuses on collecting 40 cases and converting CTA scans into an anonymous format. The subsequent analysis was carried out using the open-source software "3DSlicer" through segmentation of type B aortic dissections, encompassing both the true and false lumen. This process concludes with a description of the 16 cases segmented by the author.

By exploring different open-source software programs for segmentation and various segmentation methods, the final goal of successfully segmenting the CTA scans was achieved. Thus, the selected software tool is suitable for segmenting type B aortic dissections. Since the completed files no longer contain patient-specific data, anonymity is provided. This enables multidisciplinary teams or technicians to further use the data to develop an artificial intelligence (AI) program capable of performing automated segmentations. Although the semi-automatic segmentation process has been proven to be

rather time-consuming, the advancement of three-dimensional (3D) patient modeling as a contemporary standard in medical imaging could enable several clinical benefits [52, 55].

Automatic segmentations can contribute to visually representing complex morphologies, anatomic abnormalities, or pathologies, enabling better procedural planning and follow-up assessments. Overall, segmentations have the potential to enhance interventional procedures and provide precise sizing of stent grafts and implants. Implementing automatic segmentations could therefore not only aid clinicians in decision-making and therapeutic workflows, but also contribute to reducing workloads and enhancing risk evaluation processes in aortic care. They could serve as a dynamic tool for clinicians, enhance decision-making, and optimize patient care for aortic diseases.

In conclusion, this thesis contributes valuable insights into aortic dissection as a disease and provides an analysis through a comprehensive examination of 16 cases. The application of the open-source software “3DSlicer” for segmentation proved to be a significant advancement, showcasing future potential for enhanced diagnostics and understanding in the field of cardiac surgery, and optimized patient care for aortic diseases.

.

15. Index of literature

1. Gudbjartsson T, Ahlsson A, Geirsson A, Gunn J, Hjortdal V, Jeppsson A. Acute type A aortic dissection – a review. Scand Cardiovasc J [Internet]. 2019 [cited 2024 Jun 18] ;53(5):245-259 https://doi.org/10.1080/14017431.2019.1660401

2. Arun D, Munir W, Schmitt LV, Vyas R, Ravindran JI, Bashir M, et.al. Exploring the correlation and protective role of diabetes mellitus in aortic aneurysm disease. Front Cardiovasc Med [Internet]. 2021 [cited 2024 Jun 18];8:769343. https://doi.org/10.3389/fcvm.2021.769343

3. Dev R, Gitanjali K, Anshuman D. Demystifying penetrating atherosclerotic ulcer of aorta: unrealized tyrant of senile aortic changes. J Cardiovasc Thorac Res [Internet]. 2021 [cited 2024 Jun 18];13(2):137-143. https://doi.org/10.34172/jcvtr.2021.15

4. Greve D, Funke J, Khairi T, Montagner M, Starck C, Falk V, et at. Cocaine-related aortic dissection: what do we know? Braz J Cardiovasc Surg [Internet]. 2020 [cited 2024 Jun 18];35(6):889-896. https://doi.org/10.21470/1678-9741-2020-033

5. Sherifova S, Holzapfel GA. Biomechanics of aortic wall failure with a focus on dissection and aneurysm: A review. Acta Biomater [Internet]. 2019 [cited 2024 Jun 18];99:1-17. https://doi.org/10.1016/j.actbio.2019.08.017

6. Al'Aref SJ, Girardi L, Swaminathan RV, Lau C, Feldman DN, Gosh D, et al. A contemporary review of acute aortic dissection. Emerg Med Open Access [Internet]. 2015 [cited 2024 Jun 18];5(2):1000274. https://doi.org/10.4172/2165-7548.1000274

7. Zhang Z. Nierenarterienstenose und Nierenarterienverschluss. MSD manuals for healthcare professionals [Internet]. 2019 [cited 2024 Jun 18]. https://www.msdmanuals.com/de/profi/urogenitaltrakt/renovaskul%C3%A4re-krankheiten/nierenarterienstenose-und-nierenarterienverschluss

8. Erben Y, Oderich GS, Debus ES. Akute mesenteriale Ischämie. In: Operative und Interventionelle Gefäßmedizin. Springer Medizin e.Medpedia [Internet]. 2014 [cited 2024 Jun 18]. https://doi.org/10.1007/978-3-662-45856-3_78

9. Manninger-Wünscher M. Symptomentrack I: kardiologische Leitsymptome. VMC, Medizinische Universität Graz. 2021.

10. Kurz T. Leitsymptom: Thoraxschmerz. In: DGIM Innere Medizin. Springer Medizin e.Medpedia [Internet]. 2013 [cited 2024 Jun 18]. https://www.springermedizin.de/emedpedia/dgim-innere-medizin/leitsymptom-thoraxschmerz?epediaDoi=10.1007/978-3-642-54676-1_273

11. Strandberg K. The clinical use of a D-Dimer essay. Acutecaretesting.org [Internet]. 2017 [cited 2024 Jun 18]. Available from: https://acutecaretesting.org/-/media/acutecaretesting/files/pdf/the-clinical-use-of-a-ddimer-assay.pdf

12. Husmann M. Aortenaneurysma und -Dissektion: Pathophysiologie, Epidemiologie und Diagnostik. Z Gefäßmed [Internet]. 2015 [cited 2024 Jun 18]. Available from: https://www.kup.at/kup/pdf/12831.pdf

13. Müller S, Bonatti J, Hellweg G, Pachinger O. Erkrankungen der thorakalen Aorta: klinische Symptomatik, elektrokardiographische, röntgenologische und echokardiographische Diagnostik. J Kardiol [Internet]. 2001 [cited 2024 Jun 18]. https://www.kup.at/kup/pdf/540.pdf

14. Wong DR, Lemaire SA, Coselli JS. Managing dissections of the thoracic aorta. Am Surg. 2008 May;74(5):364-380. Author's manuscript available in PMC 2010, February 18.

15. Wallner J, Hochegger K, Chen X, Mischak I, Reinbacher K, Pau M, et al. Clinical evaluation of semi-automatic open-source algorithmic software segmentation of the mandibular bone: practical feasibility and assessment of a new course of action. PLoS One [Internet]. 2018 [cited 2024 Jun 18];13(4) https://doi.org/10.1371/journal.pone.0196378

16. Ismaguilova A, Martufi G, Gregory AJ, Appoo JJ, Herget EJ, Kotha V, et al. Multidimensional analysis of descending aortic growth after acute type A aortic dissections. Ann Thorac Surg [Internet]. 2021 [cited 2024 Jun 18];112(1):127-134. https://doi.org/10.1016/j.athoracsur.2020.04.064

17. Farber MA, Ahmad TS. Aortendissektion. MSD manuals for healthcare professionals [Internet]. 2019 [cited 2024 Jun 18]. https://www.msdmanuals.com/de/profi/herz-kreislauf-krankheiten/krankheiten-der-aorta-und-ihrer-seiten%C3%A4ste/aortendissektion

18. Schünke M, Schulte E, Schumacher U, Voll M, Wesker K. Äste der Aorta abdominalis: unpaare und indirekt paarige Äste. In: Prometheus LernAtlas - Innere Organe. 5th ed. Stuttgart: Thieme; 2018. https://doi.org/10.1055/b-006-149645

19. Amboss. Aortic dissection. Amboss. Updated 2024. Part of the Examenlehrplan for the 2nd Staatsexamen 2024. Available from: https://www.amboss.com/us/knowledge/aortic-dissection.

20. Solf MA, Gansera LS. Basics Herzchirurgie. 1st ed. Elsevier Urban & Fischer; 2012. p. 42-43. ISBN: 978-3-437-42706-0.

21. Lüllmann-Rauch R. Taschenlehrbuch Histologie. 5th ed. Thieme; 2015. p. 273-279. ISBN: 978-3-13-129245-2.

22. Hirner A, Weise K. Chirurgie. 2nd ed. Thieme; 2008. ISBN: 978-3-13-130842-9.

23. Nienaber CA, Clough RE. Management of acute aortic dissection. Lancet. 2015;385(9970):800-811. doi: 10.1016/s0140-6736(14)61005-9.

24. Bhatia S. Surgical versus endovascular repair for aortic dissection: a systematic review and meta-analysis. Eur J Cardiothorac Surg. 2018;54(3):486-494.

25. Akin I, Kische S, C. Rehders T, Nienaber C, Rauchhaus M, Ince H. Endovascular repair of thoracic aortic aneurysms. N Engl J Med. 2010 doi: 10.5114/aoms.2010.17075

26. Estrera AL, Safi HJ. Surgical repair of acute and chronic type A aortic dissections. J Thorac Cardiovasc Surg. 2006;131(3):778-790.

27. Erbel R, Aboyans V, Boileau C, Bossone E, Di Bartolomeo R, Eggebrecht H, et al. 2014 ESC guidelines on the diagnosis and treatment of aortic diseases: document covering acute and chronic aortic diseases of the thoracic and abdominal aorta of the adult. Eur Heart J. 2014;35(41):2873-2926. doi:10.1093/eurheartj/ehu281.

28. Sueyoshi E, Sakamoto I, Nakashima K, Minami K, Hayashi K. Imaging of acute aortic dissection: multi-detector row computed tomography vs magnetic resonance imaging. J Comput Assist Tomogr. 2005; 29(3):339-344. doi:10.1097/01.rct.0000159309.10612.01.

29. Fedorov A, Beichel R, Kalpathy-Cramer J, Finet J, Fillion-Robin J, Pujol S, et al. 3D Slicer as an image computing platform for the Quantitative Imaging Network. Magn Reson Imaging. 2012 ;30(9):1323-1341. doi:10.1016/j.mri.2012.05.001.

30. Ghajafrleghi R, Dessalles CA, Lal R, McCraith S, Sarathy K, Jepson N, et al. 3D Printing for Cardiovascular Applications: From End-to-End Processes to Emerging Developments. Ann Biomed Eng. 2021;49(7):1598-1618. Published online 2021 May 17. doi:10.1007/s10439-021-02784-1.

31. Jafarina A, Melito GM, Müller TS, Rolf-Pissarczyk M, Holzapfel GA, Brenn G, et al. Morphological parameters affecting false lumen thrombosis following type B aortic dissection: a systematic study based on simulations of idealized models. Biomech Model Mechanobiol. 2023. doi:10.1007/s10237-023-01687-5.

32. Tolenaar JL, Kern JA, Frederik H. Predictors of false lumen thrombosis in type B aortic dissection treated with TEVAR. Ann Cardiothorac Surg. 2014.

33. Fritz-Rößler A, Debus ES. Perioperatives Management bei Eingriffen an der Karotis und der Aorta. Dissertation. Klinikum Hamburg Eppendorf; 2021.

34. Isselbacher EM, Preventza O, Black JH III, Augoustides J, Beck A, Bolen M, et al. ACC/AHA Guideline for the Diagnosis and Management of Aortic Disease: A Report of the American Heart Association/American College of Cardiology Joint Committee on Clinical Practice Guidelines. 2022. doi: 10.1161/CIR.0000000000001106.

35. Rathore K, Newman M. Aortic Root and Distal Arch Management During Type an Aortic Dissection Repair: Expanding Horizons. Braz J Cardiovasc Surg. 2022; 37(6):921-931. doi: 10.21470/1678-9741-2021-0178.

36. Singh C, Wang X, Wong C. Importance of stent-graft design for aortic arch aneurysm repair. 2017. doi:10.3934/BIOENG.2017.1.133.

37. Hussain ST, Svensson LG. Surgical techniques in type A dissection. Ann Cardiothoracic Surg. 2016; 5(3):233-235.

38. Chaddha A, Erickson S, Kline-Rogers E, Montgomery D, Woznicki E, Jabara J, et al. Medication adherence patterns in aortic dissection survivors. 2018. doi: 10.4103/ijmr.IJMR_1198_15.

39. Martin G, Patel N, Grant Y, Jenkins M, Gibbs R, Bicknell C. Antihypertensive medication adherence in chronic type B aortic dissection is an important consideration in the management debate. 2018. doi: 10.1016/j.jvs.2017.12.063.

40. Malaisrie SC, Szeto WY, Halas M, Svensson L, Moon M. The American Association for Thoracic Surgery expert consensus document: Surgical treatment of acute type A aortic dissection. J Thorac Cardiovasc Surg. 2021;162(3).

41. Saw LJ, Lim-Cooke MS, Woodward B, Woodward B, Othman A, Harky A. The surgical management of acute type A aortic dissection: Current options and future trends. 2020. doi: 10.111/jocs.14733.

42. Liu D, Luo H, Lin S, Zhao L, Qiao C. Comparison of the efficacy and safety of thoracic endovascular aortic repair with open surgical repair and optimal medical therapy for acute type B aortic dissection: A systematic review and meta-analysis. Int J Surg. 2020. doi:10.1016/j.ijsu.2020.08.051.

43. Fattori R, Bacchi-Reggiani L, Bertaccini P, Napoli G, Fusco F, Longo M. Evolution of aortic dissection after surgical repair. Int J Cardiol. 2000. doi:10.1016/S0002-9149(00)01108-5.

44. Almeida GF, Vegni R, Japiassú AM, Kurtz P, Drumond L, Freitas M, et al. Postoperative complications of surgically treated ascending aortic dissection. 2011;23(3):304-311.

45. Han DK, Jokisch C, McKinsey JF. Expanding the Landing Zone for TEVAR: A discussion of the longevity and durability of commonly used extra thoracic debranching techniques. 2019.

46. Sayed, A., Munir, M, Bahbah, EI. Aortic Dissection: A Review of the Pathophysiology, Management and Prospective Advances. Curr Cardiol Rev. 2021;17

47. Sherk H, Khaja M, Williams W. Anatomy, Pathology, and Classification of Aortic Dissection. Tech Vasc Interv Radiol. 2021; 24:100746.

48. Slicer Community. 3D Slicer Documentation. 2023. Available from: https://slicer.readthedocs.io/_/downloads/en/latest/pdf/

49. Fernsebner MG. Technische und klinische Ergebnisse der endovaskulären Behandlung von Stenosen und Verschlüssen der Arteria subclavia. Diplomarbeit. Betreut von Deutschmann H. Ao.Univ.-Prof. Dr.med.univ.. 2009.

50. Catanho M, Sinha M, Vijayan V. Model of Aortic Blood Flow Using the Windkessel Effect. Mathematical Methods in Bioengineering. 2012

51. Oberhuber A, Raddatz A, Betge S, Ploenes C, Ito W, Janosi RA. Interdisziplinäre deutsche Leitlinien für die klinische Praxis zur Behandlung der Aortendissektion Typ B. Gefasschirurgie. 2023;28(Suppl 1):1-28. Published online: 2023 April 24. doi:10.1007/s00772-023-00995-5.

- 52. Mayer C, Pepe A, **Hossain S,** Karner B, Arnreiter M, Kleesiek J. Type B Aortic Dissection CTA Collection with True and False Lumen Expert Annotations for the Development of AI-based Algorithms. Nature. Sci Data. 2024; 11:596.
- 53. Mayer C, Arnreiter M, Karner B, **Hossain S,** Deutschmann HA, Zimpfer D. Aortic Segmentations and Their Possible Clinical Benefits. In: Segmentation of the Aorta. Towards the Automatic Segmentation, Modeling, and Meshing of the Aortic Vessel Tree from Multicenter Acquisition. 2024 p. 135-140. doi:10.1007/978-3-031-53241-2_11.
- 54. Pepe A, Li J, Rolf-Pissarczyk M, Gsaxner C, Chen X, Holzapfel G. Detection, Segmentation, Simulation and Visualization of Aortic Dissections: A Review. Med Image Anal. 2020; 65:101773. doi:10.1016/j.media.2020.101773.
- 55. Arnreiter M, Karner B, Mayer C, **Hossain S,** Pepe A, Mächler H. Utilizing Three-Dimensional Image Segmentation for Swift Evaluation of Morphology and Risk Classification in Type B Aortic Dissection. Abstract Grazer Herzkreislauftage. 2023.
- 56. Karner B, Arnreiter M, Mayer C, **Hossain S,** Mächler H, Deutschmann HA, et al. Three-dimensional Image Segmentation Permits Rapid Morphologic Assessment and Risk Stratification in Type B Aortic Dissection. Abstract ÖGHTG. 2023.
- 57. Mayer C, Pepe A, **Hossain S,** Karner B, Arnreiter M, Mächler H, et al. Segmentation of Type B Aortic Dissections with True and False Lumen for the Development of AI-based Algorithms. Abstract ÖGHTG. 2023.

58. Salameh MJ, Ratchford EV. Aortic dissection. Vasc Med. 2016;21(3):276-280. doi: 10.1177/1358863X16632898. Epub 2016 Mar 17. PMID: 26989169.

59. Universitätsklinikum Köln, Aortenchirurgie. 2024. Available from: https://herz-thoraxchirurgie.uk-koeln.de/erkrankungen-therapien/aortenchirurgie/

- Publications in connection with the project of this thesis

16. Appendix

- Ethics vote:

Medizinische Universität Graz
Ethikkommission

Auenbruggerplatz 2, A-8036 Graz
ethikkommission@medunigraz.at
Tel.: +43 / 316 / 385-13928, Fax: -14348

VOTUM
gültig bis 13.05.2023

EK-Nummer:	34-161 ex 21/22 1600-2021
Studientitel:	Creation of automatic image segmentation programmes and software-based prognostic markers concerning true and false lumen for Type B Aortic Dissection
Prüfer:	Ao.Univ.-Prof.Dr. MA MSc Heinrich Mächler Medizinische Universität Graz
Sponsor:	Medizinische Universität Graz, Abteilung für Herzchirurgie
Ansprechpartner:	Heinrich Mächler, 8036 Graz, Auenbruggerplatz 29
CRO:	-
Antragsteller:	Medizinische Universität Graz
Ansprechpartner:	Ao.Univ.-Prof. Dr.med. MA MSC Heinrich Mächler

Die o.a. Studie wurde von der Ethikkommission erstmals im 'expedited Review' am 28.12.2021 behandelt. Die Ethikkommission ist zu folgendem Schluss gekommen:

Es besteht kein Einwand gegen die Durchführung der Studie in der vorliegenden Form.

Kommissionsmitglieder, die für diesen Tagesordnungspunkt als befangen anzusehen waren und daher gemäß Geschäftsordnung an der Entscheidungsfindung und Abstimmung nicht teilgenommen haben: keine

Zur Beurteilung vorliegende Dokumente:

Dokumente eingegangen am 16.12.2021, begutachtet im 'expedited Review' am 28.12.2021	
✓ Cover Letter anschreiben-ctaorta 1.0.	15.12.2021
✓ Antragsformular ECS	16.12.2021
Originalprotokoll Studienprotokoll-CTAorta-final-version-3.1 3.1.	23.11.2021
✓ Conflict of Interest Erklärung interestconflict-ctaorta 1.0.	16.12.2021
CV 1240_2020-curriculum-vitae-cv-machler-cv-1-20200101 1.0.	01.01.2020
Dokumente eingegangen am 29.12.2021 (in der nächsten Begutachtung mitbegutachtet)	
✓ Antragsformular ECS Unterschriftenseiten	14.12.2021
Dokumente eingegangen am 21.02.2022 (in der nächsten Begutachtung mitbegutachtet)	
✓ Originalprotokoll 3.3	18.01.2022
✓ CV Prüfer 2.0	14.01.2022
✓ Sonstiges: Stellungnahme zur Bearbeitungsmitteilung	
Dokumente eingegangen am 26.03.2022 (in der nächsten Begutachtung mitbegutachtet)	
✓ Stellungnahme Prüfer	26.03.2022
Dokumente eingegangen am 10.05.2022, begutachtet im 'expedited Review' am 13.05.2022	
✓ Zahlungsbeleg	26.04.2022

Die Ethikkommission geht - rechtlich unverbindlich - davon aus, dass es sich um keine klinische Prüfung nach AMG bzw. MPG handelt.

Das Votum der Ethikkommission berührt in keiner Weise die alleinige Verantwortung der Prüferin / des

Figure 37: Ethics vote page 1, source: vote by the Ethics Committee of the Medical University of Graz

Prüfers / der Prüfer für die ordnungsgemäße Durchführung der Studie unter Einhaltung aller einschlägiger gesetzlicher Bestimmungen und Richtlinien.

Weiters machen wir darauf aufmerksam, dass der Kommission unverzüglich zu melden sind:

- Abweichungen vom Protokoll aus Sicherheitsgründen oder Protokolländerungen

- Änderungen, die das Risiko der Teilnehmer/-innen erhöhen oder die Durchführung der Studie wesentlich beeinflussen

- Mutmaßliche unerwartete schwerwiegende Nebenwirkungen - SUSARs (AMG-Studien ab 1.5.2004) oder schwerwiegende unerwünschte Ereignisse - SAEs (andere Studien)

- Jegliche Information über sonstige Umstände, die die Sicherheit der Teilnehmer/-innen oder die Durchführung der Studie beeinträchtigen können

zusätzliche Auflagen: Die behördlich vorgeschriebenen Maßnahmen hinsichtlich der COVID-19 Pandemie müssen beachtet werden. Der Prüfer und der Sponsor müssen in ihrem jeweiligen Wirkungskreis unter allfälliger Beachtung von Leitlinien gewährleisten, dass keine zur Bekämpfung der Pandemie benötigten Ressourcen gebunden werden bzw. ausreichend Personal vorhanden ist und die TeilnehmerInnen durch ihre Studienteilnahme keiner zusätzlichen Infektionsgefahr ausgesetzt werden.

Dieses Votum gilt für ein Jahr ab dem Datum der Ausstellung. Bei längerer Studiendauer ist rechtzeitig vor Ablauf der Gültigkeit des Votums ein Zwischenbericht vorzulegen (Berichtsformular), um eine etwaige Verlängerung zu erlangen.

Graz, 13. Mai 2022

Univ.Prof.DI Dr.Josef Haas
Vorsitzender

Univ.Prof.Dr.Hans Peter Dimai
Stv. Vorsitzender

Achtung: Bitte bei allen das Projekt betreffende Schreiben oder telefonischen Anfragen die EK-Nummer angeben!

Medizinische Universität Graz, Auenbruggerplatz 2, A-8036 Graz. www.medunigraz.at
Rechtsform: Juristische Person öffentlichen Rechts gem. UG 2002. Information: Mitteilungsblatt der Universität. UID: ATU 575 111 79. Bankverbindung: Raiffeisen Landesbank Steiermark IBAN: AT443800000000049010, BIC: RZSTAT2G

Figure 38: Ethics vote page 2, source: vote by the Ethics Committee of the Medical University of Graz